forests

MDPI

Review

Holocene Forest Dynamics in Western Mediterranean Islands: Rates, Periodicity, and Trends

Fabrizio Michelangeli [1,*], Elisa De Luca [1], Donatella Magri [1], Simone De Santis [1], Alessandra Celant [1], Matthieu Ghilardi [2], Matteo Vacchi [3], Jordi Revelles [4,5], Rita Teresa Melis [6], Juan Ochando [1,7], José Carrión [8], Roberta Pini [9], Gabriel Servera-Vives [10] and Federico Di Rita [1,*]

1 Department of Environmental Biology, Sapienza University of Rome, Piazzale Aldo Moro 5, 00185 Rome, Italy
2 CEREGE, CNRS-AMU-IRD-Collège de France-INRAE, 13545 Aix-en-Provence, France
3 Department of Earth Sciences, Università di Pisa, 56126 Pisa, Italy
4 Institut Català de Paleoecologia Humana i Evolució Social (IPHES-CERCA), Zona Educacional 4, Campus Sescelades URV (Edifici W3), 43007 Tarragona, Spain
5 Departament d'Història i Història de l'Art, Universitat Rovira i Virgili, Av. de Catalunya 35, 43002 Tarragona, Spain
6 Department of Chemical and Geological Sciences, University of Cagliari, Monserrato, 09042 Cagliari, Italy
7 Department of Physical Sciences, Earth and environment, University of Siena, Strada Laterina, 8, 53100 Siena, Italy
8 Department of Plant Biology (Botany Area), Faculty of Biology, University of Murcia, Campus de Espinardo, 30100 Murcia, Spain
9 Laboratory of Palynology and Palaeoecology, CNR—IGAG, Piazza della Scienza 1, 20126 Milano, Italy
10 ArqueoUIB, Departament de Ciències Històriques i Teoria de les Arts, Universitat de les Illes Balears, 07122 Palma, Spain
* Correspondence: fabrizio.michelangeli@uniroma1.it (F.M.); federico.dirita@uniroma1.it (F.D.R.)

Abstract: The forest ecosystems of large Mediterranean islands are critical hubs of evolutionary diversity with unique floristic composition and distinctive vegetation patterns reflecting long-term population dynamics and ecological legacies. Mediterranean islands provide invaluable natural archives, preserving crucial insights into the resilience of past forest ecosystems and their responses to climate variability. In this paper, we provide a comprehensive overview of the Holocene vegetation history of major western Mediterranean islands, with the twofold aim of examining the timing, extent, and rates of vegetation changes over the last few thousand years, and evaluating the influence of Rapid Climate Changes (RCCs) on forest ecosystems. The rate of change analysis allowed the identification of a distinct pattern of rapid shifts in forest composition, corresponding to periods of climate instability. These shifts align with the periodicity of Bond events, suggesting synchronicity between changes in forest ecosystems and centennial-scale climatic oscillations at a supra-regional scale. A REDFIT spectral analysis applied to palynological proxies of forest cover changes identified prominent periodicities suggesting a direct influence of solar activity and/or a relation with complex ocean–atmosphere circulation mechanisms triggered by global climate forcings.

Keywords: pollen; Holocene; rate of change; Mediterranean islands; Rapid Climate Change; Bond events

check for updates

Academic Editor: Runguo Zang

Received: 28 March 2025
Revised: 1 May 2025
Accepted: 7 May 2025
Published: 13 May 2025

Citation: Michelangeli, F.; De Luca, E.; Magri, D.; De Santis, S.; Celant, A.; Ghilardi, M.; Vacchi, M.; Revelles, J.; Melis, R.T.; Ochando, J.; et al. Holocene Forest Dynamics in Western Mediterranean Islands: Rates, Periodicity, and Trends. *Forests* **2025**, *16*, 808. https://doi.org/10.3390/f16050808

Copyright: © 2025 by the authors. Licensee MDPI, Basel, Switzerland. This article is an open access article distributed under the terms and conditions of the Creative Commons Attribution (CC BY) license (https://creativecommons.org/licenses/by/4.0/).

1. Introduction

Island ecosystems, with their unique biodiversity, are especially vulnerable to climate change and increasing human pressure: enhanced droughts, flooding events, accelerated sea level rise, coastal erosion, and changes in precipitation regime are deeply affecting the

stability of insular forest ecosystems all over the world [1–3]. At the same time, overexploitation of natural resources, agricultural expansion, mining activity, environmentally harmful development, and rising demographic demands are significantly degrading and fragmenting island ecosystems at unprecedented rates [4,5]. These stress factors severely affect plant communities, with consequences on habitat provision, vegetation composition, and ecosystem functioning [6].

Within the Mediterranean Basin, insular ecosystems constitute cradles of evolutionary diversity, contributing with high levels of endemism [7,8] to the ca. 25,000 plant species recorded [9,10]. Among them, the large western Mediterranean islands—Corsica, Sardinia, Sicily, and the Balearic Islands—occupy a transitional and climate-sensitive position, influenced by an array of large-scale atmospheric circulation mechanisms, including the subtropical high-pressure belt, the mid-latitude Westerly System, the North Atlantic Oscillation, and the Siberian High-Pressure System, among others [11]. The complex interplay of these climate drivers modulates the spatiotemporal distribution of precipitation and temperature, exerting a direct influence on Mediterranean forest ecosystems [12]. As a result, large western Mediterranean islands are particularly vulnerable to climate change, so that their ecosystems are expected to face adverse effects in relation to changing hydroclimatic conditions.

During the Holocene, the hydroclimatic variability of the western Mediterranean was driven by large-scale teleconnections of coupled atmosphere–ocean processes originating in the North Atlantic realm [13,14]. Bond et al. (2001) [15] associated nine cooling phases, marked by enhanced deposition of Ice Rafted Debris (IRD) in the North Atlantic, with quasi-periodic variations in the North Atlantic Thermohaline Circulation. In the Mediterranean realm, these phases, known as Bond events, appear as hydroclimatic oscillations determining shifts in forest stability [16,17].

Despite the growing body of palaeoecological evidence linking Bond events to environmental shifts all over the globe, the timing, extent, and causal mechanisms of these Rapid Climate Changes (RCCs) are still debated. Furthermore, the nature of a quasi-periodic "1500-year" cyclicity proposed for these climate shifts remains controversial [13,18,19]

Uncertainties in the climate signal of the Bond events and their spatiotemporal variability may arise from multiple interacting factors. These include intrinsic chronological errors in palaeoecological records and differences in sampling resolution within and across different palaeoclimatic/palaeoecological time series. Furthermore, complex meso- and local-scale hydroclimatic mechanisms interact with broader mid-latitude modes of climate variability, such as those associated with the North Atlantic-Mediterranean teleconnection patterns. In recent times, human activity added another layer of complexity, further blurring the responses of ecosystems to RCCs.

The large western Mediterranean islands, standing at the core of this highly dynamic system, are pivotal for assessing rates of change and resilience of insular forest ecosystems in relation to past climate events.

Palynological research holds remarkable value in tracing the long-term effects of climate change, the extent of human impact, and the timing of Rapid Vegetation Changes (RVCs) in isolated vulnerable ecosystems. Until the end of the 20th century, palaeovegetational research from the largest islands of the western Mediterranean mainly consisted of pioneering studies from Corsica and the Balearic Islands [20–22]. Recently, new interdisciplinary studies on lacustrine sediment cores, especially from coastal areas, and new dating techniques contributed with novel insights into the main trends in the vegetation history of Mediterranean islands and their driving factors [23–29].

Here we provide an overview of pollen records from Corsica, Sardinia, Sicily, and the Balearic Islands, with the aim of (i) examining and comparing the timing, extent,

and rates of changes in vegetation composition, (ii) identifying biogeographic patterns, and (iii) evaluating the influence of Rapid Climate Changes (RCCs) on forest ecosystems. Synthetizing data across multiple sites into a wider regional approach may allow for a better understanding of local and regional vegetation patterns, offering a cohesive narrative of past forest dynamics.

2. Materials and Methods

We retrieved 54 pollen records (Figure 1, Table S1) from western Mediterranean islands, based on the literature and online databases [30,31]. In order to perform an accurate comparative study of the vegetation dynamics, we excluded the following:

- Records for which detailed pollen counts are not available;
- Records with less than four chronological constraints (radiocarbon dates or dated tephras);
- Records spanning less than 3000 years.

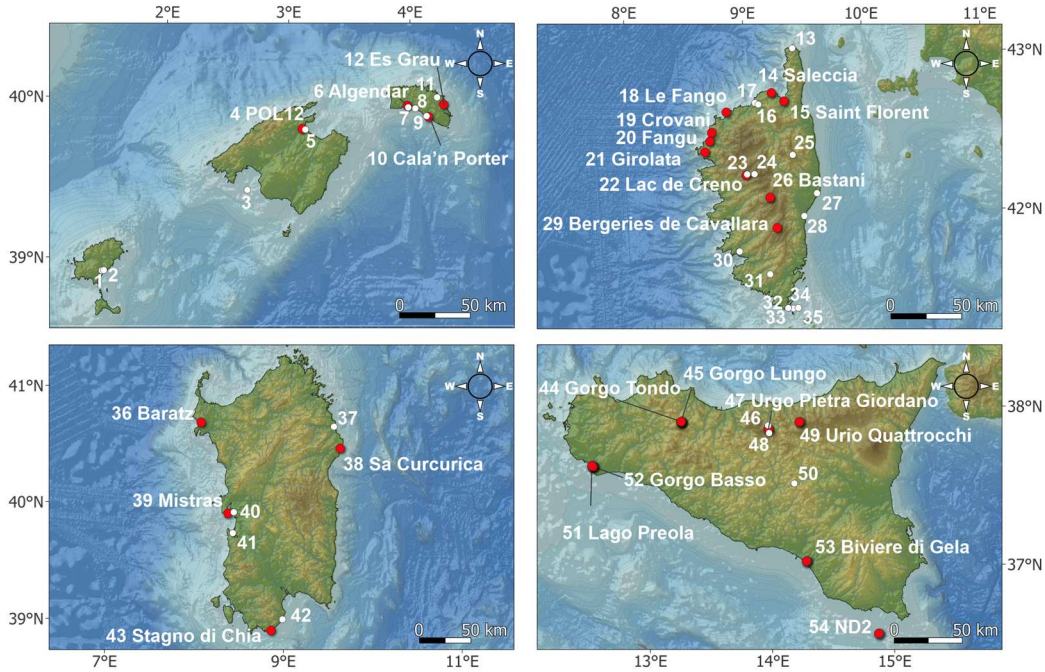

Figure 1. Map of the major western Mediterranean islands showing the published study sites from the Balearic Islands (**top left**), Corsica (**top right**), Sardinia (**bottom left**), and Sicily (**bottom right**). Red dots represent selected sites, white dots represent sites that do not fulfill the selection criteria described in Section 2 and for which pollen counts are not available (Table S1).

After applying these stringent selection criteria, we collected pollen counts and geochronological data of 25 pollen records from Sicily, Sardinia, Corsica, and the Balearic Islands.

Bayesian age-depth modeling was applied to the selected pollen records using the R package "rBacon" ver. 3.0.0 [32], to minimize the chronological uncertainty due to different calibration curves and inconsistent age estimation methods across multiple sites [33,34]. When applicable, the date of core collection was assigned to the top sediment layer, serving as additional chronological tie point. Optimal prior parameters (accumulation.shape, memory.strength, memory.mean, accumulation.rate, and thickness) were identified considering the geochronological and stratigraphic information reported in the original publications or iteratively estimated following software suggestions and model inspections (Table S2).

Pollen percentages were calculated for each pollen site on a base sum of terrestrial plants, using the Neotoma categories "TRSH" and "UPHE" (Table S3). Adopting this approach may overlook the overrepresentation of local taxa linked to site-specific envi-

ronmental conditions but guarantees a common standard for statistical analysis and data representation. Synthetic pollen diagrams were produced using the software Psimpoll 4.27 [35]. Pollen taxa were grouped into six ecological groups based on their ecological, agricultural and bioclimatic affinities, as follows: Arboreal Pollen (AP), mediterranean forest, mesophilous forest, cultivated trees (*Juglans*, *Castanea*, *Vitis*), herbs, and cereals (Table S3). *Olea* was considered separately given its dual role as a natural element of the Mediterranean maquis and a tree closely related to human activity. *Vitis* and *Castanea* may also have had a dual role, but pollen frequencies from natural stands are negligible in the studied islands.

Rate of change analysis (RoC) was performed for each selected pollen record using the R package "R-Ratepol" ver. 1.2.2 [36]. This approach provides a standardized and robust methodology for evaluating the timing and magnitude of significant compositional changes within and between pollen sequences, enabling the detection of regional and local-scale patterns in compositional rate of change [36]. We applied an age-weighted average smoothing method and adopted a moving window as working units (WUs) to minimize artifactual alterations of RoC resulting from variations in sample density and sedimentation rate [37]. Given the uneven temporal resolution of the selected pollen records and the centennial scale of the investigated vegetation dynamics and climate processes, the size of time bins was set at 200 years. To estimate RoCs, we adopted a chi-squared dissimilarity coefficient, which is particularly well-suited for dealing with closed compositional data, such as pollen percentages. In each WU, pollen counts were standardized to 150 or the lowest number detected in the dataset.

Significant shifts in RoC scores were identified using non-linear trend methods. This approach involved fitting generalized additive models (GAMs) through the RoC scores and calculating residuals as the distance between fitted and original values. Peaks in RoC scores were deemed significant if residuals exceeded at least 2 standard deviations. The proportion of peak points within 200-year time bins was calculated to assess synchronous periods of Rapid Vegetation Change. The 200-year time binning was selected based on the sampling resolution of the available pollen records, averaging 121 years. Given the constraints imposed by data density, the 200-year binning minimized the occurrence of empty bins and provided a balance between temporal resolution and data availability.

This approach allowed for the recognition of time intervals characterized by prominent changes in vegetation composition, revealing potential drivers of change across pollen sequences, also in relation to other palaeoecological and paleoclimatic proxies.

Rarefaction analysis was applied to standardize pollen counts of varying sizes across samples and estimate the number of pollen types per sample [38]. Using the PAST software ver. 4.17 [39], we calculated unbiased palynological richness to investigate diversity patterns in standardized pollen counts, including rarefaction of the Shannon H diversity index to assess dissimilarities between pollen samples, and Pielou's J metric to compare evenness among samples [39–41].

We applied a spectral analysis to AP percentages to assess periodicities in forest cover changes and to explore the possible influence of solar irradiance on forest cover dynamics. For this purpose, we performed REDFIT analysis using the PAST software ver. 4.17 [42], selecting only pollen records with at least one chronological constraint every thousand years and a time resolution per sample not exceeding 150 years, on average. These criteria minimize the methodological uncertainty highlighted by Vachula and Cheung (2023) [43].

AP% time series were fitted to an Auto-Regressive AR(1) red noise model, and a runs test (parameters: n50 = 1 segment, rectangular windows; Nsim = 1000 Monte Carlo) was applied to assess the appropriateness of the AR(1) model to characterize the record (5% significance level) [39,42]. Time series with runs outside the significance level were excluded

(see Section 3.5 for further details). In order to examine if any non-AR(1) components could be identified in the accepted time series, we set the REDFIT by selecting the Welch spectral window. We scaled the theoretical red-noise spectrum by an appropriate percentile of the $\chi 2$-probability distribution to obtain a critical false-alarm threshold. Spectral peaks exceeding the critical false-alarm level were considered significant and discussed.

The REDFIT analysis was also applied to the proportion of peak points in RoC estimates to explore possible periodicities in the occurrence of Rapid Vegetation Changes (RVCs). In addition, Continuous Wavelet Transform analysis was performed on the proportion of peaks points to identify spectral signatures that consider discontinuities and change in frequency and magnitude through time, enabling the detection of transient periodic signals in the data. The Morlet Wavelet was chosen as mother wavelet.

3. Results

The direct comparison of multiple pollen records highlights major differences in the main vegetational traits across the large islands of the Mediterranean [39], revealing unique patterns of plant composition and distribution in relation to geomorphological, environmental, and bioclimatic factors. The distinctive long-term forest dynamics for each island and their ecological legacies are summarized as follows.

3.1. Sicily

The comparative analysis of palaeoecological data reveals a highly dynamic vegetation history, with recurrent vegetation shifts and dramatic changes in forest cover throughout the Holocene. From a regional perspective, the best-dated pollen sequences highlight a clear biogeographical divide between the northern and southern sectors of the island (Figure 2), reflecting physiographic and climatic patterns. The northern sector is characterized by mesophilous vegetation, belonging to the supra- and mesomediterranean bioclimatic belt. In contrast, southern Sicily is dominated by evergreen vegetation typical of the thermomediterranean bioclimatic belt [44]. Pollen records are grouped and discussed in the light of this bioclimatic divide for a more accurate understanding of vegetation dynamics across the island.

In the northeastern sector of the island, the pollen records of Urio Quattrocchi and Urgo Pietra Giordano [23,45] depict a vegetational landscape dominated by *Fagus sylvatica* and deciduous *Quercus*, providing valuable insights into past forest dynamics of the southernmost beech populations of Europe. In these records, real forest conditions occurred only during the Early and Mid-Holocene. A general reduction in tree cover was found during the Late Holocene, with alternating phases of semi-open deciduous forest, with *Fagus*, and open environments (Figures 2 and S1). In addition to this general pattern, recurrent fluctuations in AP% reflect shifts between forested and open conditions throughout the Holocene. The record of Urio Quattrocchi, extending back to the Early Holocene, shows three drops in forest cover between 11 and 7 ka cal BP, corresponding to increases in RoC estimates and aligning with Bond events 7, 6, 5b, and 5a (Figure 3). After 7 ka cal BP, a temporary abrupt drop in AP% mainly affects deciduous vegetation. This dramatic collapse of forest cover is mirrored by a sudden increase in RoC, corresponding to a negative peak in both pollen diversity and equitability. The pollen record from Urgo Pietra Giordano, located ca. 20 km apart, shows a concurrent small decrease in AP%, pollen diversity and equitability. After this temporary event, forest rapidly recovered in both records. From approximately 6 to 5 ka cal BP a moderate decline in forest cover is observed at Urio Quattrocchi along with slightly rising RoC values. This fluctuation matches a significant peak in RoC estimates at Urgo Pietra Giordano corresponding to Bond event 4. A major drop in arboreal vegetation occurred in both records between 5 and 3.5 ka cal BP, with decreasing pollen diversity

and increasing RoC scores in concomitance with Bond event 3. After this phase of forest opening, a positive trend in AP% is detected at both sites until approximately 3 ka cal BP. This reafforestation phase, coinciding with Bond event 2b, is followed by a sudden and synchronous fall in tree cover, with increasing RoC scores and decreasing pollen diversity during Bond event 2a. The last two millennia are characterized by a gradual decline in AP% and an opposite trend for the Shannon–Wiener and Pilou indexes, encompassing the Bond events 1 and 0.

In the northwestern sector of Sicily, the sites of Gorgo Lungo and Gorgo Tondo show Late Holocene vegetation dynamics marked by repeated and abrupt shifts between sparse forests, dominated by deciduous woodlands, and substantially open landscapes [23]. These fluctuations closely reflect the overall vegetation pattern observed in the northeastern sector, except for the interval 5–4 ka cal BP, where only a limited number of samples (n = 2) are available from Gorgo Tondo, preventing a detailed vegetation reconstruction. A temporary decrease in forest cover is observed in both records around 3 ka cal BP in concomitance with the Bond event 2a, though this decline was less pronounced at Gorgo Lungo. Forest recovered to ca. 1.2 ka cal BP. During the last millennium, tree cover markedly dropped with significant changes in RoC estimates during Bond events 1 and 0.

In the southwestern sector, the coastal sites of Gorgo Basso and Lago Preola offer detailed reconstructions of a long history of sclerophyllous Mediterranean vegetation. These records converge in depicting xeric herbaceous and shrubby communities during the Early Holocene, with very low AP% corresponding to Bond event 7. A sudden spread of *Pistacia* after 10 ka cal BP, probably driven by increasing moisture in the region [46,47], corresponds to significant peaks in RoC scores at both sites. Then, a negative trend in AP% encompassed the succeeding two millennia, with an open vegetational landscape during Bond events 5a and 5b. Forested conditions were reached only after ca. 7 ka cal BP, with significant peaks in RoC estimates corresponding to a marked increase in evergreen *Quercus* and *Olea*. This forested phase, lasting until ca. 1.2 ka cal BP, is characterized by opposite fluctuations of evergreen *Quercus* and *Pistacia*, balancing the overall land cover through time (Figures 2 and S1). This repeated turnover is also highlighted by fluctuating RoC scores and pollen diversity over time, being consistent with Bond events 4, 3, 2a (Figure 3). Bond events 1 and 0 intercept a remarkable opening of the vegetational landscape.

The vegetation dynamics in the southeastern tip of the island generally match the overall pattern observed for the western coastal sites, although the vegetational landscape appears considerably more open, in relation to enhanced semi-arid climatic conditions [44,48]. A rapid increase in forest cover at Biviere di Gela [49] around 7 ka cal BP is consistent with afforestation trends at Gorgo Basso and Lago Preola. However, fully forested conditions persisted for a relatively short period (ca. 5.7–4.6 ka cal BP). Similar to SW Sicily, compositional turnovers between evergreen *Quercus*- and *Pistacia*-dominated communities drove periodic transitions from oak woodlands to xerophilous shrublands or even semi-arid open landscapes. During the Late Holocene, a general decrease in AP% is marked by repeated drops in tree cover coinciding with Bond events 3, 2a, 1, and 0. The marine pollen record ND2 supports the regional existence of extensive xeric grasslands and Mediterranean steppes, with scattered forest stands oscillating through time [50,51]. During the last few centuries, a positive trend in RoC scores marks the anthropogenic increase in *Pinus* at both Biviere di Gela and ND2.

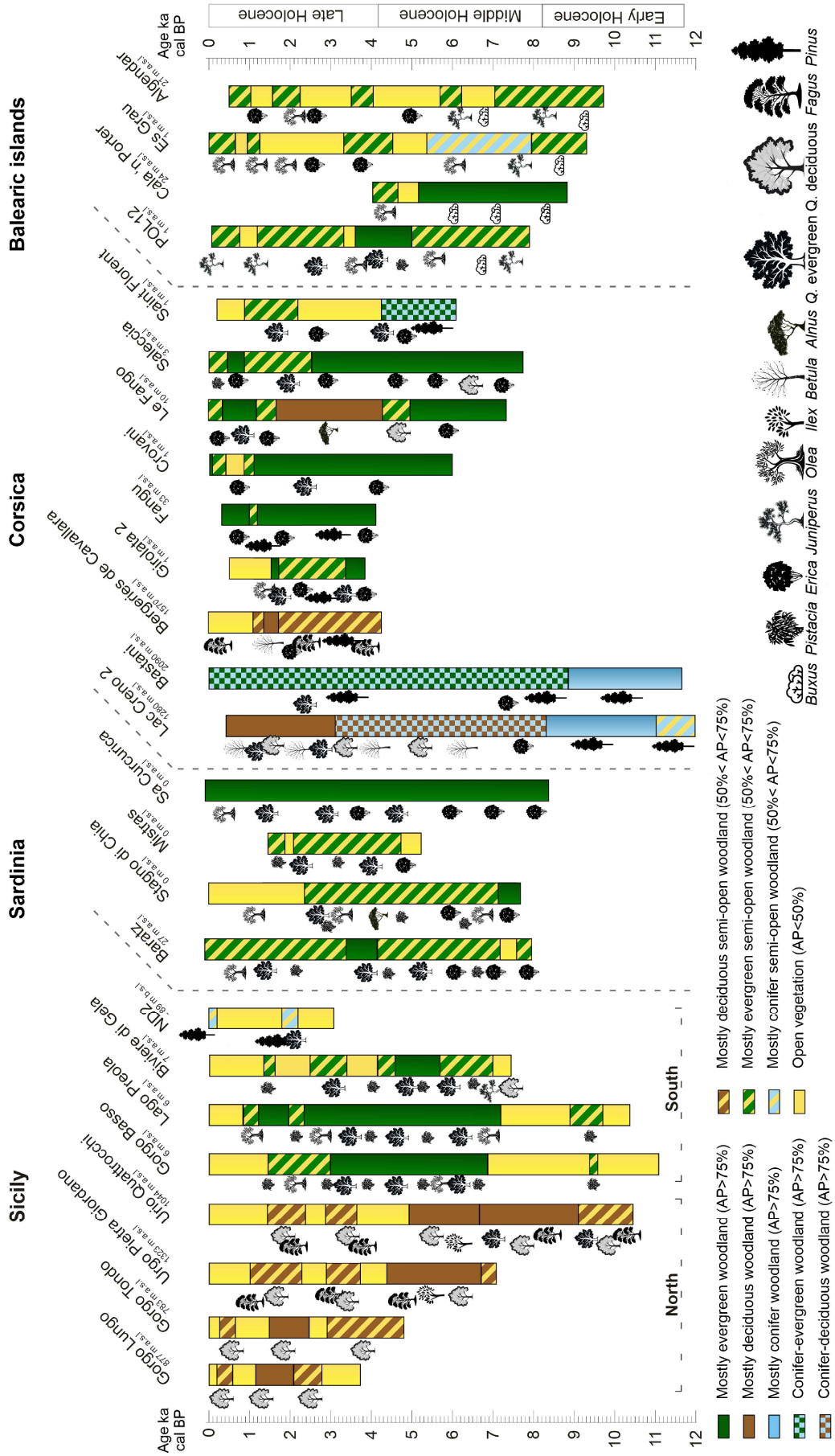

Figure 2. Scheme of the main vegetation types across the major western Mediterranean islands.

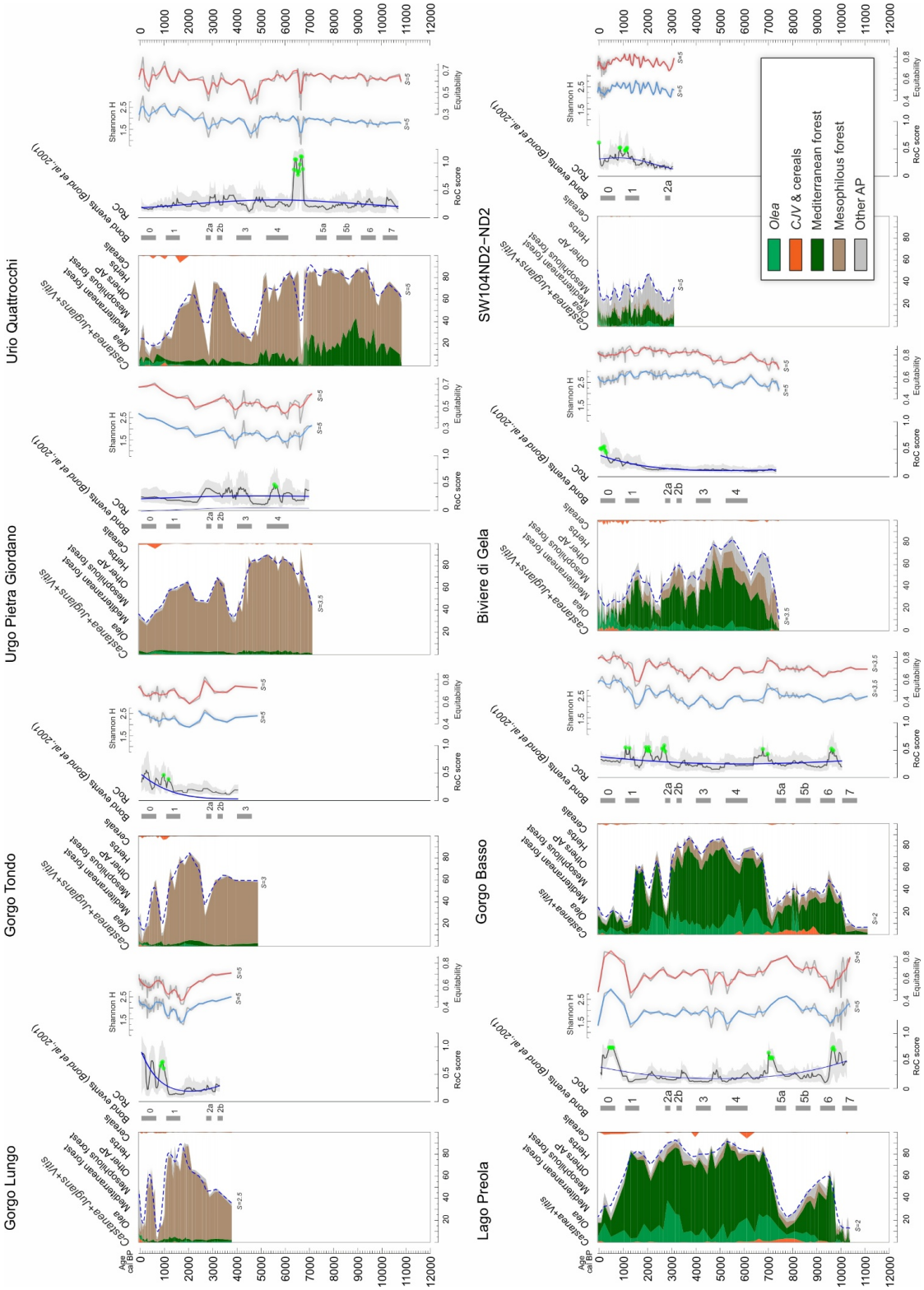

Figure 3. Synthetic pollen diagrams, rate of change (RoC) estimates, and diversity indexes in Sicily. The pollen diagrams represent cumulative percentages of cultivated trees and cereals (orange), *Olea* (pale green), Mediterranean forest (dark green), mesophilous forest (pale brown), other AP (grey), and the smoothed AP profile (dashed blue line). RoC sequences include error estimates (grey area), trends (blue line), and peak points (green dots). Shannon pollen diversity (light blue lines) and equitability (red lines) are shown both with their raw values and smoothed curves for each pollen record. The smoothing factor (S) is indicated for each curve. Numbered tiles show the timing of Bond events [15].

3.2. Sardinia

A peculiar vegetational feature for Sardinia is the persistence of extensive *Erica* woodlands, driving the ecological trajectory of the island throughout the Holocene. Although little is known about the Pleistocene and postglacial dynamics of Sardinian vegetation, the earliest evidence for the emergence of this distinctive vegetational trait can be traced back to at least the Early Holocene.

At the Early-to-Middle Holocene transition, pollen records converge in depicting a vegetation characterized by exceptionally high values of *Erica*, even exceeding 85% (Figures 2 and S1). Between 8 and 7 ka cal BP, a dramatic decline in *Erica* is first recorded at Lake Baratz, followed by Stagno di Chia [52]. This abrupt event is characterized by remarkably high RoC scores, accompanied by a sudden increase in pollen diversity and greater evenness in plant communities (Figure 4).

In the western sector of the island, the pollen record of Stagno di Sa Curcurica shows a smoother decline in *Erica*.

After 7 ka cal BP, *Erica* experienced a gradual and general decrease while remaining a major component of the vegetation (Figure S1), limiting the expansion of evergreen oak forests. This vegetation dynamics, fostering the persistence of resilient and fire-adapted scrubland communities over millennia, has been interpreted as an ecological response of Mediterranean vegetation to increased summer droughts and intensified fire regimes, in relation to enhanced seasonality during the Middle Holocene [52–56].

Between 6 and 5 ka cal BP, fluctuating percentages of *Erica* and *Pistacia,* along with low values of *Quercus*, provide a heterogenous vegetational signal across the different sectors of the island during Bond event 4. Around 5 ka cal BP, the fire-adapted scrubland communities in the eastern and western sectors of Sardinia lost ground, paving the way to *Quercus ilex* forests (Figure S1). In the south, this process appears less pronounced, with holm oaks remaining subordinate to *Erica*, and accompanied by *Pistacia*.

A direct comparison of the pollen records from Baratz and Stagno di Chia reveals that the northern and southern sectors of the island had overall opposite trends in tree cover. At Baratz, a significant increase in RoC estimates is detected from 4.2 to 3.8 ka cal BP, corresponding to the maximum AP% values of the sequence. At the same time, at Stagno di Chia a phase of tree cover decline is recorded. High RoC scores are observed at both sites between 3.4 and 2.7 ka cal BP, encompassing the time of Bond Events 2a and 2b. This phase coincides with a decrease in tree cover at Baratz and an increase at Stagno di Chia. No significant changes are found at Mistras and Sa Curcurica, located at the western and eastern coasts of Sardinia, respectively.

During the last 2000 years, the palaeoecological record shows diverging trajectories in the studied pollen sites, with a progressive reduction in trees at Baratz and Stagno di Chia, with the last being more open, while Sa Curcurica remains forested (Figure 4).

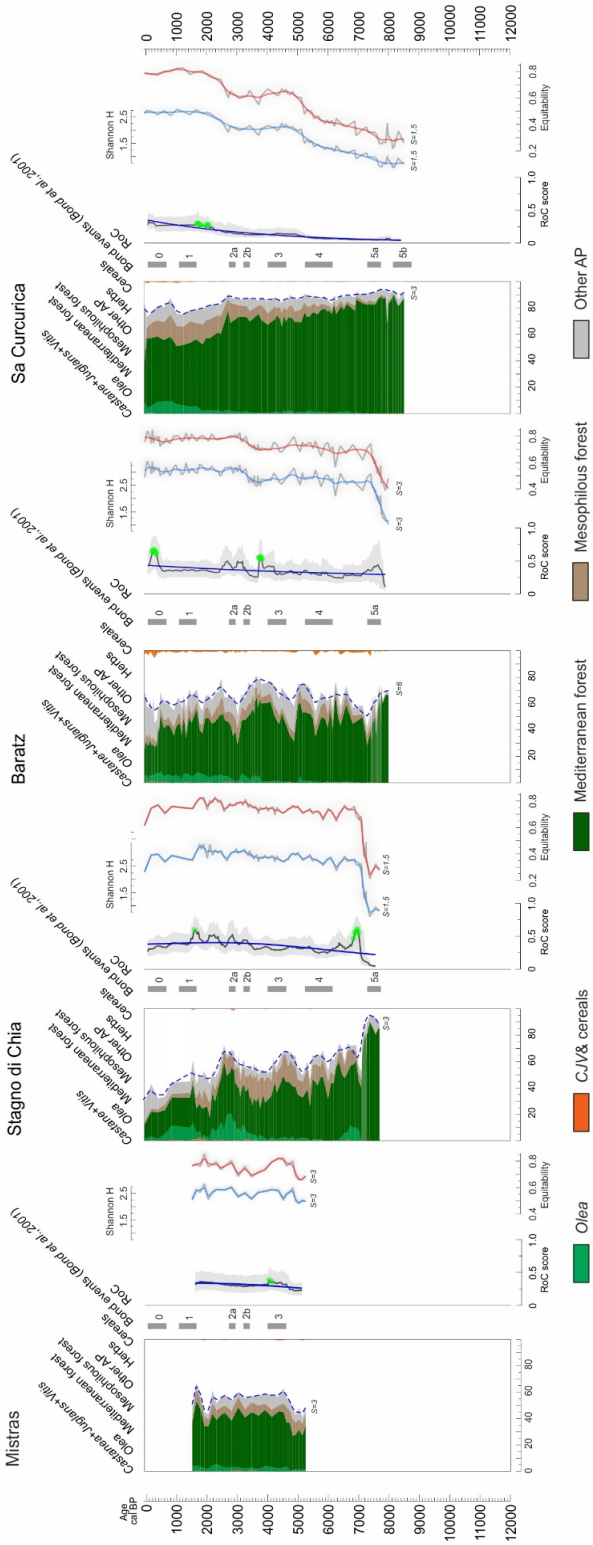

Figure 4. Synthetic pollen diagrams, rate of change (RoC) estimates, and diversity indexes in Sardinia. The pollen diagrams represent cumulative percentages of cultivated trees and cereals (orange), *Olea* (pale green), Mediterranean forest (dark green), mesophilous forest (pale brown), other AP (grey), and the smoothed AP profile (dashed blue line). RoC sequences include error estimates (grey area), trends (blue line), and peak points (green dots). Shannon pollen diversity (light blue lines) and equitability (red lines) are shown both with their raw values and smoothed curves for each pollen record. The smoothing factor (S) is indicated for each curve. Numbered tiles show the timing of Bond events [15].

3.3. Corsica

Corsica stands out as one of the richest Mediterranean islands in terms of palaeoecological records, especially during the Late and Mid-Holocene. At the onset of the Holocene, the pollen records of Lac de Creno and Bastani reveal a steppe phase in the mountain sector of the island, dominated by *Artemisia*, *Pinus nigra* subsp. *laricio*, and *Alnus alnobetula* (Figure 2). This floristic configuration reflects the palaeoecological legacy of the Younger Dryas, which determined cold and arid climatic conditions at the highest elevations of the island. During the Early Holocene, a general increase in tree cover is observed in the hinterland, which appears substantially unresponsive to Bond events 8, 7, and 6 (Figure 5). At ca. 8 ka cal BP, a sudden increase in *Erica arborea* marks a vegetational breakpoint confirmed by significant peaks in RoC values at Bastani (Figures 5 and S1). A concurrent, though less pronounced, increase in tree heath is recorded at Lac de Creno. The timing and extent of this expansion of *Erica* corresponds to the spread observed in Sardinia, highlighting a synchronous vegetation change at a supra-regional scale, possibly reflecting increasing temperature and humidity, as also suggested by the occurrence of *Taxus* at Lac Creno 2 and the co-occurrence of *Ulmus* and *Corylus* at Bastani Lake (Figure S1). After this pulse, there is a decline in the percentage of heath, that has remained stable at low values up to the present.

Additional pollen records are available for the Mid-Holocene, providing evidence for vegetation features in the coastal sector [20,25,27,28,57,58]. They are characterized by the pervasive presence of *Erica* woodlands, which persisted even during the development of evergreen oak forest. In coastal areas, *Erica* and *Quercus* often display opposite behaviors, showing a dynamic balance similar to that of Sardinia. This common pattern may reflect either competition between the two species [20] or a response to sustained fire regimes, enhanced seasonality, and unstable climatic conditions, promoting the persistence of *Erica*-dominated tall shrublands [59].

During the Mid-Holocene, counterbalancing oscillations in *Erica* and *Quercus* pollen resulted in relatively stable AP% at Saleccia, Saint Florent, and Crovani. In contrast, the record of Le Fango highlights two temporary openings of the forest. The first, mostly due to a decline in *Pinus*, was centered at 6.5 ka cal BP. The second occurred around 4.5 ka cal BP and was associated with increasing RoC scores and pollen diversity. These oscillations align with Bond events 4 and 3 (Figure 5).

During the Late Holocene, *Pinus* was the main component of mountain vegetation, while deciduous elements, namely *Quercus*, *Fagus*, and *Betula*, occupied lower altitudinal belts of the hinterland. The coastal sector exhibits complex dynamics, with repeated openings in tree cover, suggesting unstable environmental conditions across multiple sites (Figure 2). Significant peaks in RoC values are observed at the Mid-to-Late Holocene transition at Le Fango, corresponding to decreasing pollen diversity and equitability, as well as to a rapid increase in AP%, mainly *Erica*, *Alnus*, and *Pinus* (Figure S1). In contrast, a decrease in AP% is recorded at Saint Florent, along with a peak in RoC scores coinciding with Bond event 3. This shift reflects the local expansion of salt-tolerant vegetation, mainly Amaranthaceae, due to the local development of a lagoon system [25]. However, a similar rise in Amaranthaceae is also observed in other pollen records from Corsica, which suggests increasing aridity at a regional scale [20,25,60].

Another phase of vegetation change is observed around 3 ka cal BP, coinciding with Bond events 2a and 2b. However, diverse directions of changes are recorded throughout Corsica, possibly in relation to human activity and the heterogeneity of physiography, producing distinct microclimates. Diverse patterns of vegetation changes are also observed during the last 2000 years, showing significant shifts in RoC scores and in pollen diversity indexes (Figure 5), intercepting Bond events 1 and 0.

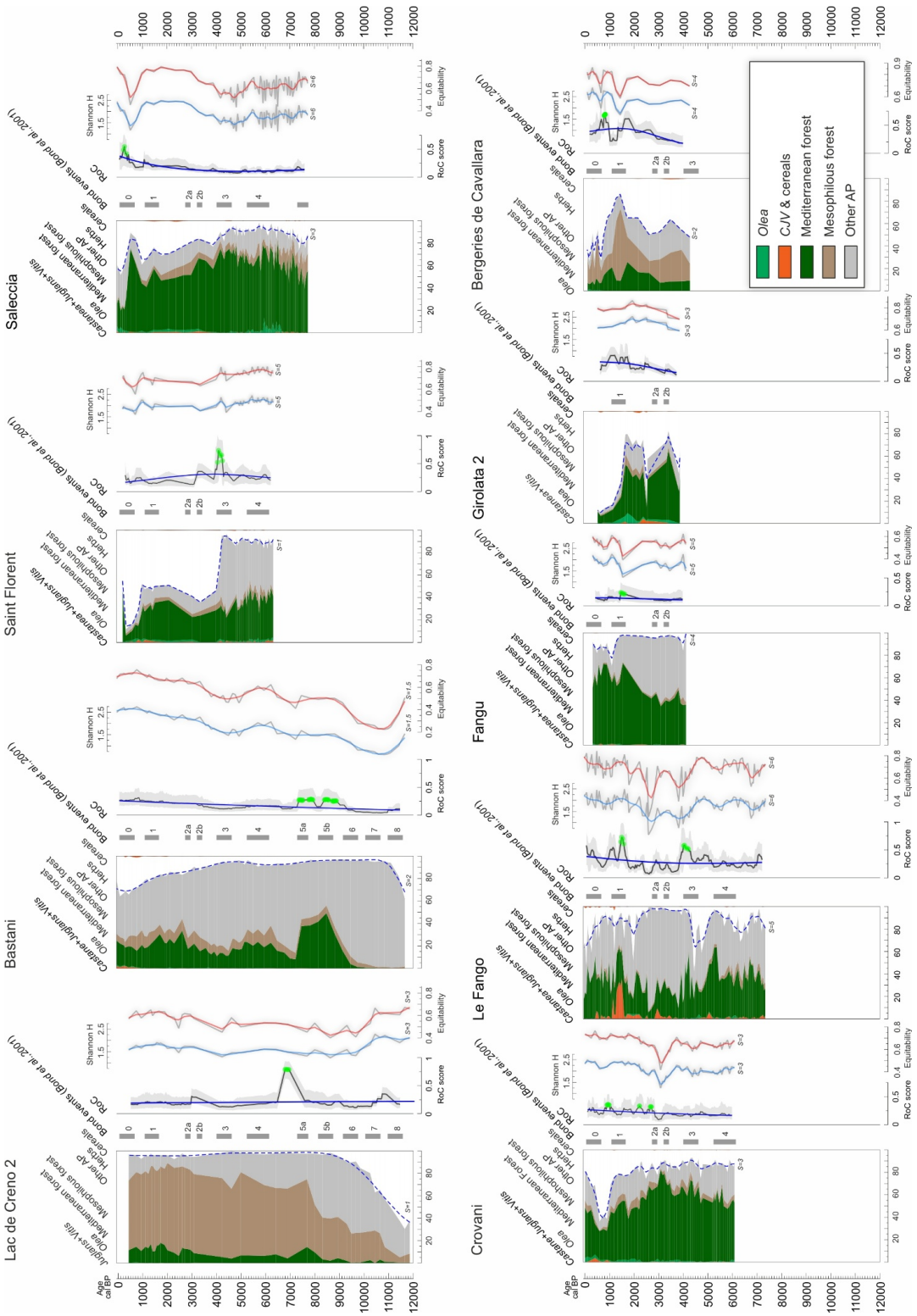

Figure 5. Synthetic pollen diagrams, rate of change (RoC) estimates, and diversity indexes in Corsica. The pollen diagrams represent cumulative percentages of cultivated trees and cereals (orange), *Olea* (pale green), Mediterranean forest (dark green), mesophilous forest (pale brown), other AP (grey), and the smoothed AP profile (dashed blue line). RoC sequences include error estimates (grey area), trends (blue line), and peak points (green dots). Shannon pollen diversity (light blue lines) and equitability (red lines) are shown both with their raw values and smoothed curves for each pollen record. The smoothing factor (S) is indicated for each curve. Numbered tiles show the timing of Bond events [15].

3.4. Balearic Islands

Pollen records from the Balearic Islands indicate a moderately forested vegetational landscape throughout the Mid- and Late Holocene [24,29]. Recurrent oscillations in the tree cover punctuated the vegetation history of the islands, resulting in alternating phases of xerophilous grasslands and evergreen semi-open woodlands. Since ca. 4 ka cal BP, the formation of mosaic landscapes was connected to human activities and drier climate conditions [61].

A distinctive trait in the vegetation composition of the archipelago is represented by pronounced pollen percentages of *Buxus* during the Early and Mid-Holocene, likely corresponding to the endemic species *Buxus balearica*. Currently, the distribution of this species includes the Balearic Islands, southern Spain, Morocco, Algeria, Turkey, and a single population located in southwestern Sardinia [62]. In the Balearic archipelago, scattered populations of Balearic boxwood occupy the calcareous slopes of Majorca and Cabrera, while it is considered extirpated from Minorca and Ibiza [63].

The restricted and fragmented distribution of this circum-Mediterranean relict, as well as the limited size of its populations across the Mediterranean Basin, suggest range contractions and progressive regional extirpation. At the genus level, the post-glacial dynamics of *Buxus* shows a trend towards gradual disappearance from regions of Southern Europe [62].

Pollen records from Minorca, where *Buxus* is no longer present, reveal a clear phase of boxwood expansion documented in three out of the four available records, encompassing the Early and Mid-Holocene [22,24]. *Buxus* percentages averaged around 20% at the Es Grau and Algendar sites and exceeded 50% in the Calan' Porter record (Figure S1). In Majorca, a coeval *Buxus* expansion is found in the POL12 pollen record from the Albufera Natural Park, though with lower frequencies [64].

At Algendar, the *Buxus*-dominated vegetation underwent a two-step reduction with sharp declines at 8 and 7 ka cal BP, respectively. This depletion corresponds to a significant peak in RoC estimates, indicating a rapid compositional shift around 7 ka cal BP, accompanied by a negative trend in overall pollen diversity and evenness (Figure 6). Between 6 and 5 ka cal BP, an abrupt vegetational shift is recorded across the Gymnesian islands (Majorca and Minorca), characterized by a sudden decrease in both boxwood and juniper and a concomitant increase in *Olea* and Ericaceae. Significant peaks in RoC estimates, observed at Calan' Porter, Albufera Alcúdia (POL12), and Es Grau, along with relatively stable values of pollen diversity and evenness, indicate a major vegetational turning point that led to the establishment of a new maquis-type landscape, which persisted throughout the Late Holocene (Figures 6 and S1). The archaeological evidence for pre-Chalcolithic visits to the Balearics is minimal, yet human-driven landscape transformation may have occurred before the islands were permanently settled [29,65]. This long history of human activity may have concurred to the contraction of *Buxus* population. All the same, a notable drop in AP% (Figure 6) aligns with the 5.2 ka event [24], indicating a temporary but significant decrease in tree cover during Bond event 4.

Between 5 and 4 ka cal BP, a general forest recovery encompasses the time span of Bond event 3, corresponding to significant peaks in RoC estimates at Algendar and Es Grau, alongside temporary slight increases in pollen diversity and evenness.

In the interval 4–2 ka cal BP, RoC analysis reveals no significant change. Stable values are observed for pollen diversity and evenness. During this period, a minor oscillation in AP% can be detected at the time of Bond event 2b, especially at POL12 and Es Grau.

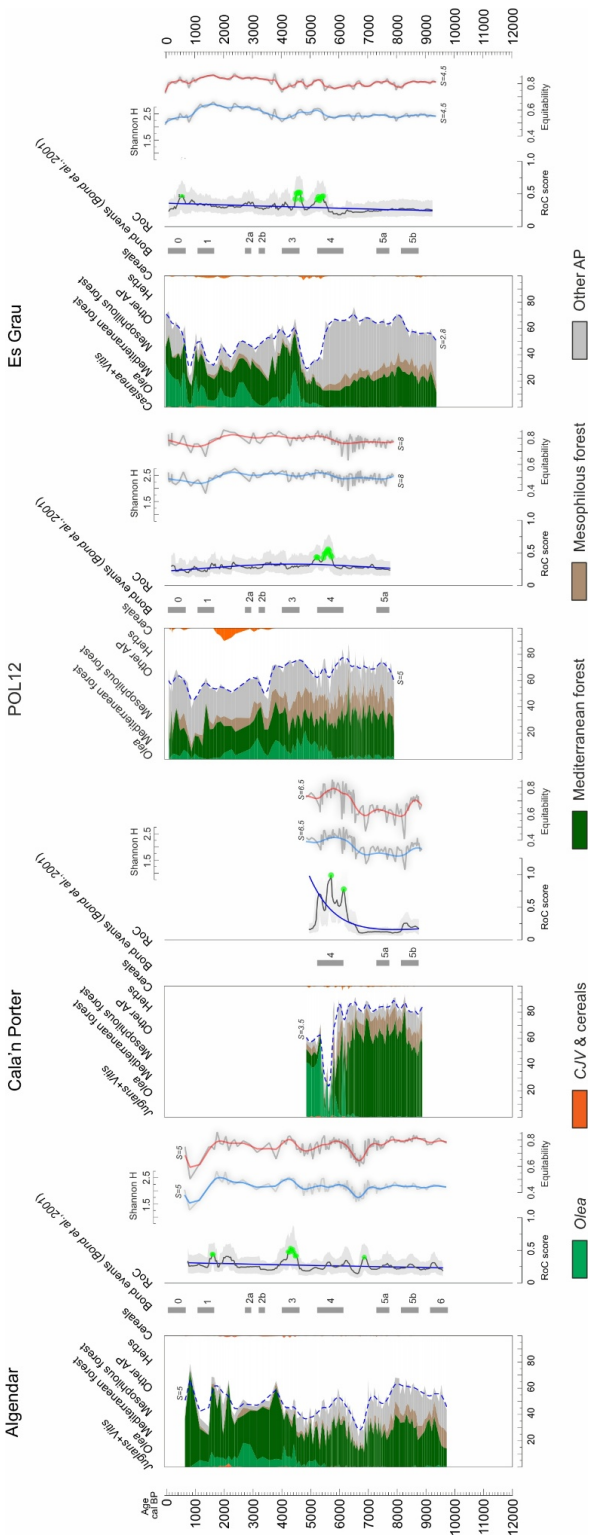

Figure 6. Synthetic pollen diagrams, rate of change (RoC) estimates, and diversity indexes in the Balearic Islands. The pollen diagrams represent cumulative percentages of cultivated trees and cereals (orange), *Olea* (pale green), Mediterranean forest (dark green), mesophilous forest (pale brown), other AP (grey), and the smoothed AP profile (dashed blue line). RoC sequences include error estimates (grey area), trends (blue line), and peak points (green dots). Shannon pollen diversity (light blue lines) and equitability (red lines) are shown both with their raw values and smoothed curves for each pollen record. The smoothing factor (S) is indicated for each curve. Numbered tiles show the timing of Bond events [15].

During the last two millennia, slightly diachronic oscillations in AP% are observed across the available pollen records from Minorca and Majorca. At Algendar, a rapid change in pollen composition is accompanied by a negative trend in pollen diversity between 1.7 and 0.8 ka cal BP, with a marked reduction in AP% corresponding to Bond event 1. At Es Grau, a negative peak in AP% aligns with a minimum in pollen diversity at around 1.0 ka cal BP. In the last millennium, forest recovered, showing a significant compositional change around 0.5 ka cal BP. A similar vegetation trend is found in Majorca, where the POL12 sequence records a drop in AP% around 1.0 ka cal BP, followed by a positive trend of tree cover during the last millennium.

3.5. REDFIT Analysis of the AP Time Series

A runs test was carried out on the AP time series of Baratz, Bastani, Biviere di Gela, Calan' Porter, Crovani, Es Grau, Fangu, Gorgo Basso, Gorgo Tondo, ND2, POL-12, Sa Curcurica, Saint Florent, Stagno di Chia, Urgo Pietra Giordano, and Urio Quattrocchi, whose pollen records meet the selection criteria discussed in Material and Methods. The runs tests indicate that the AR(1) models are appropriate to characterize 11 out of 16 records. Among them, significant periodicities were detected in the following time series: POL12 (runs = 24; 5% acceptance interval = 23–29), Crovani (runs = 16; 5% acceptance interval = 10–16), Biviere di Gela (runs = 24; 5% acceptance interval = 18–33), and Gorgo Basso (runs = 15; 5% acceptance interval = 15–23) (Figure 7).

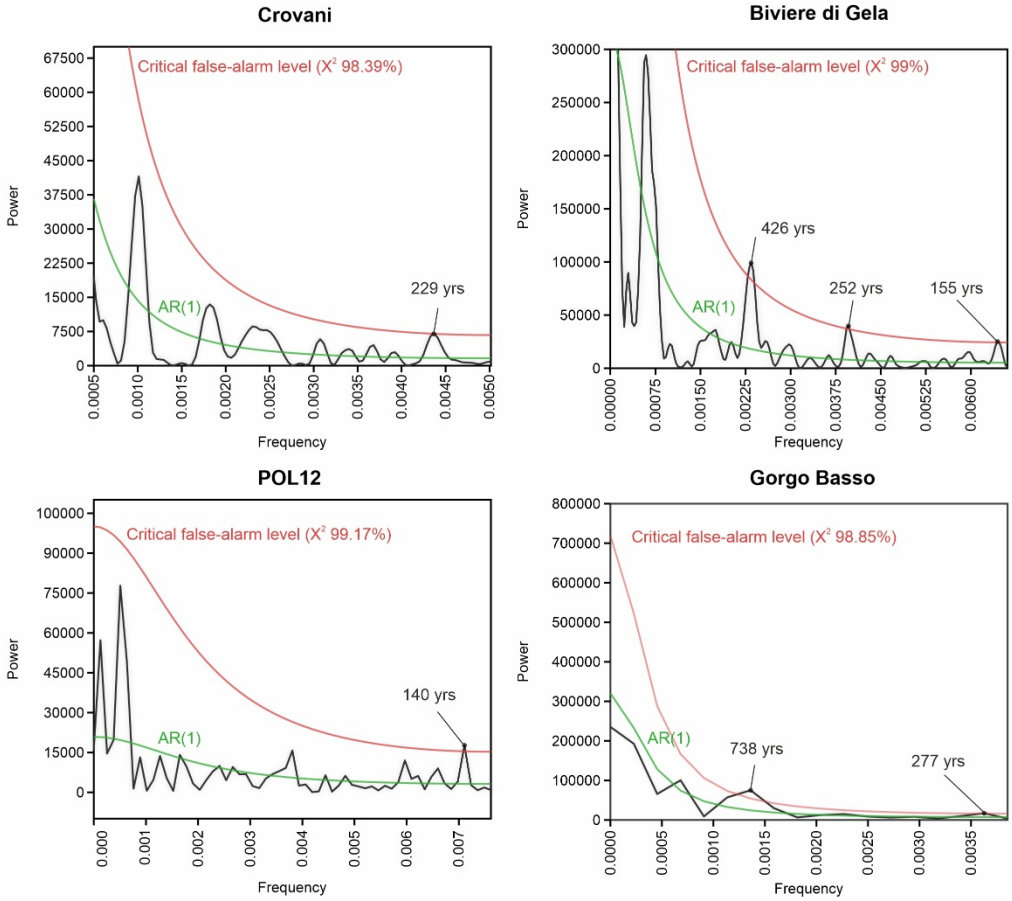

Figure 7. REDFIT analysis of the Crovani, Biviere di Gela, POL12, and Gorgo Basso records. The periodicity (years) is reported for each significant spectral peak.

In the POL12 pollen record, one spectral peak at ~140 years (frequency 0.0071092) exceeds the critical false-alarm level of 99.17%. In the pollen record from Crovani, a

spectral peak at ~230 years (frequency 0.004368) exceeds the critical false-alarm level of 98.39%. At Biviere di Gela, three spectral peaks exceeded the critical false alarm level of 99% at ~420 years (frequency 0.0023461), ~250 years (frequency 0.0039653), and ~150 years (frequency 0.0064436). In the pollen record from Gorgo Basso, two spectral peaks of ~740 years (frequency 0.001355) and ~270 years (frequency 0.0036124) exceed the critical false alarm level of 98.85%. The significant periodicities detected have a time interval that is at least twice the average time resolution of the corresponding time series.

4. Discussion

4.1. Rate of Change Analysis and Rapid Climate Changes (RCCs)

The Holocene vegetation history of the major Mediterranean islands reveals an extremely complex scenario, marked by significant variability in insular vegetation dynamics at both regional and supra-regional scales. Remarkable challenges arise from low dating density, intrinsic dating error, heterogenous and/or sparse sampling resolution, and uneven spatial distribution of pollen records. In such historically dynamic regions, the rise, demise, trade, and shifts of ancient civilizations make it hard to discern between the relative impact of human activities and climatic factors.

Despite these sources of uncertainty, accurate vegetation reconstructions from multiple sites allow tracing the main ecological trajectories in western Mediterranean islands and identifying drivers of change including human activity and climate variability [23–25,66,67]. The indisputable role of human impact in causing major landscape transformations has been extensively explored, especially in the Middle and Late Holocene [45,49,53,59,68,69], while the role of centennial-scale climate fluctuations remains largely underexplored. In this regard, Burjachs et al. (2017) [24] made a pioneering investigation to assess the role of RCCs in determining abrupt vegetation shifts in the Balearic Islands, and highlighted the correspondence of minima in mesic forests with Bond events. In Sicily, the marine pollen record ND2 revealed regional short-term declines in forest cover that are consistent with Bond events during the last 3000 years [51]. Furthermore, the marine record from the Gulf of Gaeta in central Italy [17,70] shows a clear correspondence of vegetation shifts with the quasi-periodic signal of Bond events. Beyond these tentative efforts, vegetation changes documented in pollen records from Corsica, Sardinia, Sicily, and the Balearic Islands have not been properly examined in terms of recurrent climatic events.

The RoC analysis provides evidence for statistically significant Rapid Vegetation Changes (RVCs), punctuating the environmental history of large Mediterranean islands (Figure 8). Peaks in RoC estimates offer valuable insights into the timing and rates of vegetation changes, capturing abrupt shifts in species composition that may not be evident in overall forest cover, as highlighted by AP%.

From an overall perspective, RVCs are not evenly distributed through time. The temporal distribution of significant peaks in RoC estimates reveals an increasing frequency from the Early Holocene to the present. This pattern likely results from a combination of factors, including the increasing human impact on forest ecosystems, a greater availability of pollen data in the Middle and Late Holocene compared to the Early Holocene (orange line in Figure 8a), and enhanced sensitivity of forests to intensifying climatic dryness and seasonality variability during this period [71–73].

Starting from the Middle Holocene, when an appreciable number of sites fulfill the selection criteria, the pattern in the proportion of peak points reveals a noticeable correspondence between periods of high frequency of RVCs (red and green lines in Figure 8b) and peaks in the geochemical signature of Ice Rafted Debris (IRD) corresponding to Bond events (blue line in Figure 8b). The proportion of peak points associated with decreasing forest cover (red line in Figure 8b) aligns with IRD maxima of Bond events 4, 3, 2a, 1, and

0. The profile of peak points related to no substantial changes in tree cover (dashed line in Figure 8b) shows a similar pattern, with the exception of the interval 8.5–7 ka cal BP, where a cluster of peaks corresponds with Bond event 5. The peak points coinciding with increasing tree cover (green line in Figure 8b) show an overall opposite trend.

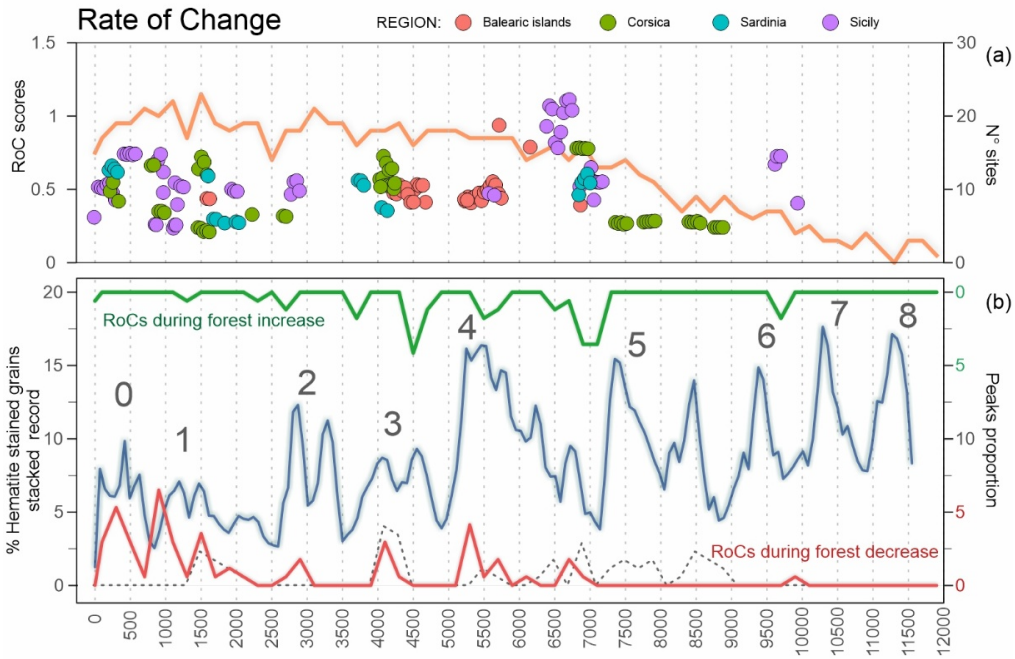

Figure 8. Temporal distribution of statistically significant peaks in RoC scores. (**a**) Dots indicate RoC scores for the Balearic Islands (red), Corsica (green), Sardinia (blue), and Sicily (purple). The orange line shows the number of sites represented in 200-yr time bins. (**b**) Proportion of significant peaks in RoC scores (200-yr time bins) during forest decreases (red line), increases (green line), and stability (dashed line). The blue line shows the IRD variability through time [15].

Individual sites exhibit varied responses, with prominent compositional shifts during some Bond events while remaining stable during others. The response of insular Mediterranean forests to these climatic events may have been more nuanced than a uniform and coherent trajectory, reflecting varying degrees of resilience, adaptation, local ecological processes, and site-specific vegetation dynamics. Rather than triggering synchronous and widespread forest cover changes, these climatic fluctuations appear to have influenced the pace of compositional changes. This applies particularly to Corsica and Sardinia, where dynamic and compensatory equilibria between *Erica*-dominated shrublands and evergreen oak forests resulted in a relative stability of AP% through time (Figure S1). This long-term opposite behavior finds a modern parallel in Sardinia, where the ongoing aridification led to the retreat of evergreen holm oak forest, fostering the expansion of *Erica*-dominated shrublands [74]. The concurrent drought-triggered dieback of evergreen forests and the expansion of bushy heath vegetation during the last century may represent a good analogue for past RCVs, suggesting increasing aridity during Bond events.

In Sicily, a more direct correspondence was found between Bond events and the decline in forest cover (Figure S1), reflecting a higher sensitivity of forest ecosystems to centennial climatic conditions and consequently greater environmental vulnerability compared to Corsica and Sardinia. This vulnerability may largely depend on a greater exposure of Sicily to the northward migration of high-pressure cells from North Africa with respect to other western Mediterranean islands, as highlighted by synoptic studies on past climate events [75–78]. The indisputable role of a long-term human occupation, documented by archaeological sites and pollen records, may have exacerbated tree cover

oscillations throughout the Holocene. However, the peaks in RoC estimates detected during the Early Holocene, and coinciding with the arrival of the first Neolithic communities to Sicily, correspond to a significant forest increase that cannot be ascribed to the human spread of cultivated trees (Figure 3). Human activity was more likely a factor contributing to tree cover and compositional changes in later periods, particularly during the Middle and, especially, the Late Holocene, when a better correspondence between RoC estimates, tree cover decrease, and cereals occurrences can be observed.

In the Balearic Islands, RVCs concentrate substantially around Bond events 4 and 3, intercepting substantial vegetational reorganization linked to the decline of *Buxus* and *Juniperus* and the setting of mediterranean forest dominated by *Erica* and *Olea*. These changes may have been amplified and accelerated by human activities during the 6th millennium cal BP, when first sporadic occupations could have occurred, even before the definitive human settlement in the 5th millennium BP.

Considering all the islands together, a consistent temporal pattern is evident. Without implying any climatic determinism, the temporal alignment of RVCs with Bond events suggests that shifts in hydroclimatic conditions significantly contributed to rapid transformations in the structure and composition of insular forest ecosystems, acting in conjunction with human impact.

Further insights into the influence of climate events on insular forests composition emerge from the REDFIT analysis, which reveals a significant millennial-scale periodicity of 1344 years (Figure 9), aligning with the cyclicity of ~1374 ± 502 years observed in IRD concentrations for the Holocene [79]. This result is also supported by Continuous Wavelet Transform analysis, highlighting a consistent periodic signal in the proportion of RoC peaks (Figure 9). The detection of this cyclicity strengthens the hypothesis that long-term climatic rhythms played a key role in shaping ecological resilience and forest composition, providing further context for understanding the climatic forces driving forest cover changes in large western Mediterranean islands.

4.2. Fundamental Tempo of Forest Cover Variability

The REDFIT test applied to the AP time series for the identification of the fundamental tempo in forest cover changes reveals statistically significant periodicities that are described as follows.

The periodicity of ~740 years found at Gorgo Basso has never been investigated before in the Mediterranean Basin. Evidence of this periodicity was found in flood records of the Southern Alps influenced by North Atlantic Oscillation variability [80]. In the marine domain, periodicities of ~740–750 years were recently detected by Le Houedec et al. (2024) [81] in Planktonic foraminiferal $\delta^{18}O$ signals from both western and eastern Mediterranean records, as well as from a central Mediterranean record, 80 km apart from Gorgo Basso in the Sicily Strait [82]. Periodicities of 800–700 years, particularly well expressed in North Atlantic marine records, were attributed to the pacing activity of Atlantic Meridional Overturning Circulation (AMOC) on oceanic circulation [83]. According to Dima and Lohmann (2009) [84], these periodicities, as well as those of ~1400–1500 years underlying the cold Bond climate events [79], may derive from a rectification of an external solar forcing possibly operated by the Termohaline Circulation (THC), which may explain their recurrence in palaeoclimate and palaeoceanographic records at the global scale [85,86]. In particular, the variability of the AMOC component of the THC is documented to play an influence on climate processes of the Mediterranean [87–89]. The periodicity of ~740 years found at Gorgo Basso supports climate teleconnections between North Atlantic and Sicily highlighted by previous investigations [17,51].

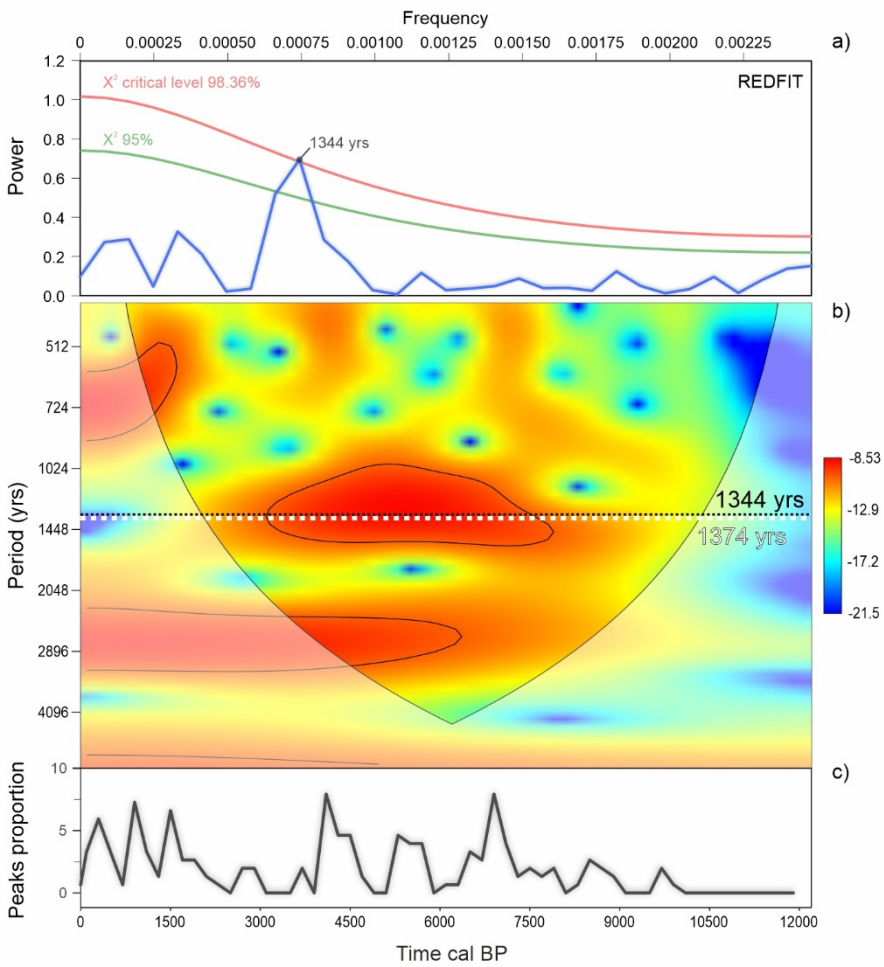

Figure 9. (**a**) REDFIT spectral analysis of the proportion of peak points through time. The 95% confidence levels of the critical level of χ2 are reported on the graph with a green line and a red line. (**b**) Wavelet transform of peaks proportion. The white shaded area indicates the cone of influence. Signal power is shown with a red–blue gradient. The black contour indicated the significance level corresponding to $p = 0.05$. The dashed black line corresponds to the period identified by REDFIT analysis and the white dashed line is the periodicity of Bond events for the Holocene [79]. (**c**) Total proportion of RoC peak points within 200-yr time bins.

The ~420-year cycle found at Biviere di Gela was detected in direct proxies of solar activity. This periodicity may relate to the oscillatory mode of the Sun's convective zone, and was identified in ^{14}C time series [90]. According to Damon and Jirikowic (1992) [91], it may represent a harmonic overtone of the Hallstatt cycle (2100–2500 years). The ~420 cycle was identified in several palaeoenvironmental records connected to hydroclimatic changes, especially in North America [92], but in Mediterranean countries it was rarely recorded. For example, a cycle of 430 years was detected by Sabatier et al. (2020) [93] in the records of total solar irradiance, although the authors attribute a low climatic significance to this cycle. A similar periodicity was found in $\delta^{13}C$ records of speleothems from Northern Iberia, where it was interpreted as the result of climate forcing mechanisms related to changes in solar irradiance and North Atlantic circulation patterns [94].

The ~270-year periodicity found at Biviere di Gela is in line with the ~270-year cycle found by Degeai et al. (2015) [95] in a storminess record of the northwestern Mediterranean from a sedimentary sequence of the Gulf of Lion. Degeai et al. (2015) [95] argue that this cycle appears coherent with the total solar irradiance record. This indicates that the Late Holocene multi-centennial variability of cyclogenesis in the western Mediterranean was steered by an external solar-driven climate forcing. Although the origin of the ~270-year

periodicity is still unclear, the influence of the El Nino Southern Oscillation (ENSO) as causation of this cycle cannot be ruled out. A similar peak of frequency was also detected by Azuara et al. (2020) [96] in the coherency analyses of the ENSO variability with both the Gulf of Lion Sea Surface Temperature and TERR-Alkanes. Although the authors interpret this specific centennial peak as spurious, they support a clear influence of the ENSO climate variability over the Mediterranean. Outside the Mediterranean, a 270-yr periodicity was detected by Gao et al. (2023) [97] in paleoenvironmental records of Northern China and was attributed to the influence of ENSO in regulating the intensity of the East Atlantic Summer Monsoon. Regardless of the periodicity of 270 years, Piervitali and Colacino (2001) [98] revealed a correspondence between phases with a higher (lower) number of drought events in Sicily and phases with a lower (higher) number of ENSO events.

The 250-year periodicity found at Biviere di Gela was identified in direct proxies of solar activity [99,100]. This peak of frequency is consistent with periodicities of ~250–260 years recorded in various palaeoclimatic proxies of hydrological changes at the middle and high latitudes of the Northern Hemisphere [80,101–105], as well as in the Mediterranean Basin [106,107]. Swindles et al. (2012) [105] suggest that 250–260-year periodicities may reflect quasi-periodic signals of the Suess solar cycle, since they fall in the bandwidth of this fundamental solar cyclicity [100], or a combination of the Suess cycle and the Gleissberg cycle.

The ~230-year cycle found at Crovani was also detected in direct proxies of solar magnetic activity, such as ^{14}C time series and historical observations of sunspots [90,108], and in palaeoclimate and palaeoenvironmental time series worldwide [109–111]. According to Ron et al. (2012) [112], this periodicity may reflect the influence of the Suess cycle on Earth rotation and have major implications for climate systems. In the Mediterranean Basin, a prominent ~230-yr cycle was found in several abundance records of the placolith species *Florisphaera profunda* [113 and references therein]. According to Incarbona et al. (2023) [113], solar variability is a main climatic forcing for water column and phytoplankton dynamics during the preindustrial age in the western Mediterranean Sea. The periodicity found by Incarbona in the Balearic Sea and that found at Crovani may be both tightly connected to ocean–atmospheric coupling mechanisms influencing the northwestern Mediterranean climate. In particular, this cycle may reflect the influence of total solar irradiance in modulating the Gulf of Lion gyre activity and the associated atmospheric circulation that determines hydroclimatic changes also in the western sectors of Corsica [114–116].

Cyclicities of ~150 and ~140 years, found at POL12 and Biviere di Gela, respectively, may be linked with direct proxies of solar activity. A ~150-year cyclicity was detected in a long ^{14}C time series [90,100] and replicated in palaeoclimate and paleoenvironmental sequences from the Northern Hemisphere, [80,117–121], especially in temperature records. Also, the 140-year periodicity may be related to solar activity, being included in the bandwidth of the Gleissberg cycle, which has a wide frequency band with a double structure consisting of 50–80-year and 90–140-year periodicities [100]. Ptitsyna & Demina (2021) [122] suggest that the 140-year cycle is the result of frequency modulation of the Gleissberg cycle operated by the Suess cycle. Foraminiferal and sedimentological time series from marine cores in the northeastern Arabian Sea revealed the 140-year periodicity along with other solar activity periodicities (~250 and 230 years) mentioned above. These were attributed to the impact of solar insolation on the southwest monsoon trends during the Holocene [123]. However, the ~140-year and ~150-year cyclicities do not present analogues in other palaeoclimate and palaeoenvironmental records of the Mediterranean Basin.

Of note, solar cycles found in AP time series of large islands were also detected in paleoclimate proxies, reflecting centennial scale shifts of the Intertropical Convergence

Zone (ITCZ) [124], whose variability has major implications in regulating hydrological changes at low and middle latitudes [18].

5. Conclusions

The comparison of multiple pollen records from large western Mediterranean islands provides a comprehensive understanding of past forest dynamics, with a focus on the timing and drivers of Rapid Vegetation Changes:

- The RoC analysis proved to be a powerful tool for detecting rapid changes in vegetation composition that may not be apparent in changes in tree cover. This approach is effective in identifying past vegetation responses to RCCs in large Mediterranean islands, especially where compensatory vegetation dynamics between oak woodlands and shrublands/heathlands may result in near-stable AP percentages over time.
- The timing of rapid changes in forest composition detected across large Mediterranean islands is consistent with centennial-scale hydroclimatic oscillations linked to Bond events. This correspondence highlights a teleconnection between the North Atlantic climate system and western Mediterranean forest ecosystems, suggesting that shifts in ocean–atmosphere mechanisms may have influenced regional hydroclimatic conditions.
- The response of insular Mediterranean ecosystems to these climate events could have been more complex, with varying degrees of resilience and adaptation depending on local factors and ecosystem characteristics.
- The spectral analysis carried out on RoC and AP time series revealed periodicities that have already been identified in paleoclimate and palaeoenvironmental records worldwide. Most of them (140–150, 230–250, and 420 years) are related to the influence of solar activity, possibly in relation to its effect on latitudinal shifts of ITCZ and the consequent reorganization of climate patterns. Other periodicities (270, 740, and 1350 years) may derive from fundamental modes of solar activity through a rectification operated by complex oceanic–atmospheric circulation mechanisms possibly involving AMOC, ENSO, and NAO, whose influence in climate variability of the Mediterranean regions is well known.

In conclusion, climate influence on Holocene vegetation dynamics in the Mediterranean realm constitutes a pressing research target in the light of current ecosystems vulnerability. Understanding the rate of change and resilience of forest ecosystems to abrupt changes in hydroclimatic conditions is crucial for developing nature conservation plans and promoting adaptation strategies specifically tailored to island ecosystems [125]. However, the impact of RCCs on Mediterranean insular vegetation is still an underexplored topic and further research on the spatiotemporal expression of centennial-scale climatic oscillations is still needed.

Supplementary Materials: The following supporting information can be downloaded at: https://www.mdpi.com/article/10.3390/f16050808/s1, Figure S1: Synthetic pollen percentage diagrams of the 25 selected sites from large western Mediterranean islands. Red lines and green circles indicate peaks in RoCs estimates. Mediterranean forest in green, mesophilous forest in brown, herbs in yellow, cultivated trees and cereals in orange. Additional magnification of low-value curves is indicated in the labels (×5); Table S1:Pollen records from large Mediterranean islands; Table S2: Selected pollen records; Table S3: Plant taxa and relative Neotoma categories used in main ecological groups.

Author Contributions: Conceptualization, F.M., E.D.L. and F.D.R.; methodology, F.M., E.D.L., F.D.R.; software, F.M. and E.D.L.; validation, J.O., F.D.R., A.C., S.D.S. and D.M.; formal analysis, F.M., E.D.L. and F.D.R.; investigation, F.M., E.D.L., F.D.R., S.D.S.; resources, M.V., M.G., J.R., G.S.-V., R.T.M.; data curation, F.M., E.D.L., J.O., S.D.S.; writing—original draft preparation, F.M., E.D.L. and F.D.R.; writing—review and editing, F.M., D.M., A.C., R.P., J.C. and F.D.R.; visualization, F.M., E.D.L., J.O. and S.D.S.; supervision, D.M., J.C., R.P. and F.D.R.; project administration, F.M., E.D.L. and F.D.R.; funding acquisition, F.D.R., A.C. and D.M. All authors have read and agreed to the published version of the manuscript.

Funding: We acknowledge financial support under the National Recovery and Resilience Plan (NRRP) funded by the European Union, NextGenerationEU, Mission 4, Component 1, CUP B53D23023560001; Project Title "TrAcking Long-term declIne of forest biodiVErsity in Italy to support conservation actions (ALIVE)", as a PRIN project of the Ministry of University and Research (MUR). This paper is also a contribution to the Sapienza University project 'HumAN and climAtic iMplicatioNs of palaEoecological changeS in large ISlands in the central Mediterranean (ANAMNESIS)'—Code: RM1221816B963D12, CUP: B83C22008590005. J.O. and J.C. thank funding by Spanish Agencia Estatal de Investigación Project PID2022-136832NB-100.

Data Availability Statement: Data will be made available on request.

Acknowledgments: We are grateful to all data contributors and data stewards of the Neotoma Palaeoecology Database.

Conflicts of Interest: The authors declare no conflicts of interest.

References

1. Harter, D.E.V.; Irl, S.D.H.; Seo, B.; Steinbauer, M.J.; Gillespie, R.; Triantis, K.A.; Fernández-Palacios, J.-M.; Beierkuhnlein, C. Impacts of Global Climate Change on the Floras of Oceanic Islands—Projections, Implications and Current Knowledge. *Perspect. Plant Ecol. Evol. Syst.* **2015**, *17*, 160–183. [CrossRef]
2. Taylor, S.; Kumar, L. Global Climate Change Impacts on Pacific Islands Terrestrial Biodiversity: A Review. *Trop. Conserv. Sci.* **2016**, *9*, 203–223. [CrossRef]
3. Médail, F. The Specific Vulnerability of Plant Biodiversity and Vegetation on Mediterranean Islands in the Face of Global Change. *Reg. Environ. Chang.* **2017**, *17*, 1775–1790. [CrossRef]
4. Mcleod, E.; Bruton-Adams, M.; Förster, J.; Franco, C.; Gaines, G.; Gorong, B.; James, R.; Posing-Kulwaum, G.; Tara, M.; Terk, E. Lessons from the Pacific Islands—Adapting to Climate Change by Supporting Social and Ecological Resilience. *Front. Mar. Sci.* **2019**, *6*, 289. [CrossRef]
5. Fernández-Palacios, J.M.; Kreft, H.; Irl, S.D.H.; Norder, S.; Ah-Peng, C.; Borges, P.A.V.; Burns, K.C.; De Nascimento, L.; Meyer, J.-Y.; Montes, E.; et al. Scientists' Warning—The Outstanding Biodiversity of Islands Is in Peril. *Glob. Ecol. Conserv.* **2021**, *31*, e01847. [CrossRef]
6. Heywood, V.; Culham, A. The Impacts of Climate Change on Plant Species in Europe. Report T-PVS/Inf9E. In *Convention on the Conservation of European Wildlife and Natural Habitats, Proceedings of the 29th Meeting of the Standing Committee, Bern, Switzerland, 23–26 November 2009*; University of Reading: Reading, UK, 2009.
7. Medail, F.; Quezel, P. Hot-Spots Analysis for Conservation of Plant Biodiversity in the Mediterranean Basin. *Ann. Mo. Bot. Gard.* **1997**, *84*, 112–127. [CrossRef]
8. Médail, F. Plant Biogeography and Vegetation Patterns of the Mediterranean Islands. *Bot. Rev.* **2022**, *88*, 63–129. [CrossRef]
9. Quézel, P. *The Study of Groupings in the Countries Surrounding the Mediterranean: Some Methodological Aspects*; Mediterranean-type shrublands; Elsevier: Amsterdam, The Netherlands, 1981; pp. 87–93.
10. Vogiatzakis, I.N.; Mannion, A.M.; Sarris, D. Mediterranean Island Biodiversity and Climate Change: The Last 10,000 Years and the Future. *Biol. Conserv.* **2016**, *25*, 2597–2627. [CrossRef]
11. Lionello, P.; Malanotte-Rizzoli, P.; Boscolo, R.; Alpert, P.; Artale, V.; Li, L.; Luterbacher, J.; May, W.; Trigo, R.; Tsimplis, M.; et al. The Mediterranean Climate: An Overview of the Main Characteristics and Issues. In *Developments in Earth and Environmental Sciences*; Lionello, P., Malanotte-Rizzoli, P., Boscolo, R., Eds.; Elsevier: Amsterdam, The Netherlands, 2006; Volume 4, pp. 1–26. ISBN 1571-9197.
12. Lionello, P. *The Climate of the Mediterranean Region: From the Past to the Future*; Elsevier: London, UK, 2012; ISBN 978-0-12-416042-2.
13. Zielhofer, C.; Köhler, A.; Mischke, S.; Benkaddour, A.; Mikdad, A.; Fletcher, W.J. Western Mediterranean Hydro-Climatic Consequences of Holocene Ice-Rafted Debris (Bond) Events. *Clim. Past* **2019**, *15*, 463–475. [CrossRef]

14. Rousseau, D.-D.; Bagniewski, W.; Ghil, M. Abrupt Climate Changes and the Astronomical Theory: Are They Related? *Clim. Past* **2022**, *18*, 249–271. [CrossRef]
15. Bond, G.; Kromer, B.; Beer, J.; Muscheler, R.; Evans, M.N.; Showers, W.; Hoffmann, S.; Lotti-Bond, R.; Hajdas, I.; Bonani, G. Persistent Solar Influence on North Atlantic Climate During the Holocene. *Science* **2001**, *294*, 2130–2136. [CrossRef] [PubMed]
16. Pèlachs, A.; Julià, R.; Pérez-Obiol, R.; Soriano, J.M.; Bal, M.-C.; Cunill, R.; Catalan, J. Potential Influence of Bond Events on Mid-Holocene Climate and Vegetation in Southern Pyrenees as Assessed from Burg Lake LOI and Pollen Records. *Holocene* **2011**, *21*, 95–104. [CrossRef]
17. Di Rita, F.; Fletcher, W.J.; Aranbarri, J.; Margaritelli, G.; Lirer, F.; Magri, D. Holocene Forest Dynamics in Central and Western Mediterranean: Periodicity, Spatio-Temporal Patterns and Climate Influence. *Sci. Rep.* **2018**, *8*, 8929. [CrossRef] [PubMed]
18. Wanner, H.; Buetikofer, J. Holocene Bond Cycles: Real or Imaginary. *Geografie* **2008**, *113*, 338–349. [CrossRef]
19. Bradley, R.S.; Bakke, J. Is There Evidence for a 4.2 Ka BP Event in the Northern North Atlantic Region? *Clim. Past* **2019**, *15*, 1665–1676. [CrossRef]
20. Reille, M. New Pollen-Analytical Researches in Corsica: The Problem of *Quercus ilex* L. and *Erica arborea* L., the Origin of *Pinus halepensis* Miller Forests. *New Phytol.* **1992**, *122*, 359–378. [CrossRef]
21. Burjachs, F.; Pérez-Obiol, R.; Roure, J.M.; Julià, R. Dinámica de La Vegetación Durante El Holoceno En La Isla de Mallorca. In *Trabajos de Palinología Básica y Aplicada*; Universitat de València: València, Spain, 1994; pp. 199–210.
22. Yll, E.-I.; Perez-Obiol, R.; Pantaleon-Cano, J.; Roure, J.M. Palynological Evidence for Climatic Change and Human Activity during the Holocene on Minorca (Balearic Islands). *Quat. Res.* **1997**, *48*, 339–347. [CrossRef]
23. Tinner, W.; Vescovi, E.; van Leeuwen, J.F.N.; Colombaroli, D.; Henne, P.D.; Kaltenrieder, P.; Morales-Molino, C.; Beffa, G.; Gnaegi, B.; van der Knaap, W.O.; et al. Holocene Vegetation and Fire History of the Mountains of Northern Sicily (Italy). *Veg. Hist. Archaeobot.* **2016**, *25*, 499–519. [CrossRef]
24. Burjachs, F.; Pérez-Obiol, R.; Picornell-Gelabert, L.; Revelles, J.; Servera-Vives, G.; Expósito, I.; Yll, E.-I. Overview of Environmental Changes and Human Colonization in the Balearic Islands (Western Mediterranean) and Their Impacts on Vegetation Composition during the Holocene. *J. Archaeol. Sci. Rep.* **2017**, *12*, 845–859. [CrossRef]
25. Revelles, J.; Ghilardi, M.; Rossi, V.; Currás, A.; López-Bultó, O.; Brkojewitsch, G.; Vacchi, M. Coastal Landscape Evolution of Corsica Island (W. Mediterranean): Palaeoenvironments, Vegetation History and Human Impacts since the Early Neolithic Period. *Quat. Sci. Rev.* **2019**, *225*, 105993. [CrossRef]
26. Carrión, J.S.; Munuera, M.; Ochando Tomás, J.; López-Sáez, J.A.; Casas-Gallego, M.; González-Sampériz, P.; Badal, E.; Pérez-Díaz, S.; Carrión-Marco, Y.; Jiménez-Moreno, G.; et al. *Paleoflora and Paleovegetation of Iberia III: Holocene*; Universidad Politécnica de Cartagena, Ministerio de Ciencia e Innovación y Fundación Séneca: Cartagena, Spain, 2022; ISBN 978-84-17853-89-1.
27. Ghilardi, M.; Revelles, J.; Mary, J.-B.; Rita, F.D.; Delhon, C.; Delanghe, D.; Robresco, S. Mid- to Late-Holocene Coastal Morphological Evolution, Vegetation History and Land-Use Changes of the Porto Gulf UNESCO World Heritage Site and Its Surroundings (NW Corsica Island, Western Mediterranean). *Holocene* **2023**, *33*, 1023–1044. [CrossRef]
28. Ghilardi, M.; Revelles, J.; Fagel, N.; Schmidt, S.; Delanghe, D. Reconstructing the Mid- to Late Holocene Human-Environments Interactions in Cape Corsica (Corsica Island, Western Mediterranean) Based on Sedimentology, Pollen Analyses and Geochemistry. *J. Archaeol. Sci. Rep.* **2025**, *62*, 104985. [CrossRef]
29. Servera-Vives, G.; Riera, S.; Picornell-Gelabert, L.; Moffa-Sánchez, P.; Llergo, Y.; Garcia, A.; Mus-Amezquita, M.; García Álvarez, S.; Calvo Trías, M. The Onset of Islandscapes in the Balearic Islands: A Study-Case of Addaia (Northern Minorca, Spain). *Palaeogeogr. Palaeoclimatol. Palaeoecol.* **2018**, *498*, 9–23. [CrossRef]
30. Williams, J.W.; Grimm, E.C.; Blois, J.L.; Charles, D.F.; Davis, E.B.; Goring, S.J.; Graham, R.W.; Smith, A.J.; Anderson, M.; Arroyo-Cabrales, J.; et al. The Neotoma Paleoecology Database, a Multiproxy, International, Community-Curated Data Resource. *Quat. Res.* **2018**, *89*, 156–177. [CrossRef]
31. Fyfe, R.M.; de Beaulieu, J.-L.; Binney, H.; Bradshaw, R.H.W.; Brewer, S.; Le Flao, A.; Finsinger, W.; Gaillard, M.-J.; Giesecke, T.; Gil-Romera, G.; et al. The European Pollen Database: Past Efforts and Current Activities. *Veg. Hist. Archaeobot.* **2009**, *18*, 417–424. [CrossRef]
32. Blaauw, M.; Christen, J.A. Flexible Paleoclimate Age-Depth Models Using an Autoregressive Gamma Process. *Bayesian Anal.* **2011**, *6*, 457–474. [CrossRef]
33. Blaauw, M.; Christen, J.A.; Bennett, K.D.; Reimer, P.J. Double the Dates and Go for Bayes—Impacts of Model Choice, Dating Density and Quality on Chronologies. *Quat. Sci. Rev.* **2018**, *188*, 58–66. [CrossRef]
34. Li, C.; Postl, A.K.; Böhmer, T.; Cao, X.; Dolman, A.M.; Herzschuh, U. Harmonized Chronologies of a Global Late Quaternary Pollen Dataset (LegacyAge 1.0). *Earth Syst. Sci. Data* **2022**, *14*, 1331–1343. [CrossRef]
35. Bennett, K. *Psimpoll' and 'Pscomb': C Programs for Analysing Pollen Data and Plotting Pollen Diagrams (Version 4.27)*; The 14Chrono Centre, Archaeology and Palaeoecology, Queen's University of Belfast: Belfast, UK, 2009.
36. Mottl, O.; Grytnes, J.-A.; Seddon, A.W.R.; Steinbauer, M.J.; Bhatta, K.P.; Felde, V.A.; Flantua, S.G.A.; Birks, H.J.B. Rate-of-Change Analysis in Paleoecology Revisited: A New Approach. *Rev. Palaeobot. Palynol.* **2021**, *293*, 104483. [CrossRef]

37. Mottl, O.; Flantua, S.G.A.; Bhatta, K.P.; Felde, V.A.; Giesecke, T.; Goring, S.; Grimm, E.C.; Haberle, S.; Hooghiemstra, H.; Ivory, S.; et al. Global Acceleration in Rates of Vegetation Change over the Past 18,000 Years. *Science* **2021**, *372*, 860–864. [CrossRef]
38. Birks, H.J.B.; Line, J.M. The Use of Rarefaction Analysis for Estimating Palynological Richness from Quaternary Pollen-Analytical Data. *Holocene* **1992**, *2*, 1–10. [CrossRef]
39. Hammer, Ø.; Harper, D.A. Past: Paleontological Statistics Software Package for Educaton and Data Anlysis. *Palaeontol. Electron.* **2001**, *4*, 1.
40. Chao, A.; Gotelli, N.J.; Hsieh, T.C.; Sander, E.L.; Ma, K.H.; Colwell, R.K.; Ellison, A.M. Rarefaction and Extrapolation with Hill Numbers: A Framework for Sampling and Estimation in Species Diversity Studies. *Ecol. Monogr.* **2014**, *84*, 45–67. [CrossRef]
41. Xie, S.; Li, K.; Li, F.; Yang, X.; Reitalu, T. Modern Pollen–Plant Diversity Relationships for Reliable Pollen-Based Reconstruction of Past Plant Taxonomic and Functional Diversity: A Case Study in Southwest Shandong, China. *Ecol. Indic.* **2024**, *167*, 112739. [CrossRef]
42. Schulz, M.; Mudelsee, M. REDFIT: Estimating red-noise spectra directly from unevenly spaced paleoclimatic time series. *Comput. Geosci.* **2002**, *28*, 421–426. [CrossRef]
43. Vachula, R.S.; Cheung, A.H. A Meta-Analysis of Studies Attributing Significance to Solar Irradiance. *Earth Space Sci.* **2023**, *10*, e2022EA002466. [CrossRef]
44. Bazan, G.; Marino, P.; Guarino, R.; Domina, G.; Schicchi, R. Bioclimatology and Vegetation Series in Sicily: A Geostatistical Approach. *Ann. Bot. Fenn.* **2015**, *52*, 1–18. [CrossRef]
45. Bisculm, M.; Colombaroli, D.; Vescovi, E.; van Leeuwen, J.F.N.; Henne, P.D.; Rothen, J.; Procacci, G.; Pasta, S.; La Mantia, T.; Tinner, W. Holocene Vegetation and Fire Dynamics in the Supra-Mediterranean Belt of the Nebrodi Mountains (Sicily, Italy). *J. Quat. Sci.* **2012**, *27*, 687–698. [CrossRef]
46. Tinner, W.; van Leeuwen, J.F.N.; Colombaroli, D.; Vescovi, E.; van der Knaap, W.O.; Henne, P.D.; Pasta, S.; D'Angelo, S.; La Mantia, T. Holocene Environmental and Climatic Changes at Gorgo Basso, a Coastal Lake in Southern Sicily, Italy. *Quat. Sci. Rev.* **2009**, *28*, 1498–1510. [CrossRef]
47. Calò, C.; Henne, P.D.; Curry, B.; Magny, M.; Vescovi, E.; La Mantia, T.; Pasta, S.; Vannière, B.; Tinner, W. Spatio-Temporal Patterns of Holocene Environmental Change in Southern Sicily. *Palaeogeogr. Palaeoclimatol. Palaeoecol.* **2012**, *323–325*, 110–122. [CrossRef]
48. Grassa, F.; Favara, R.; Valenza, M. Moisture Source in the Hyblean Mountains Region (South-Eastern Sicily, Italy): Evidence from Stable Isotopes Signature. *Appl. Geochem.* **2006**, *21*, 2082–2095. [CrossRef]
49. Noti, R.; van Leeuwen, J.F.N.; Colombaroli, D.; Vescovi, E.; Pasta, S.; La Mantia, T.; Tinner, W. Mid- and Late-Holocene Vegetation and Fire History at Biviere Di Gela, a Coastal Lake in Southern Sicily, Italy. *Veg. Hist. Archaeobot.* **2009**, *18*, 371–387. [CrossRef]
50. Michelangeli, F.; Di Rita, F.; Lirer, F.; Lubritto, C.; Bellucci, L.G.; Cascella, A.; Bonomo, S.; Margaritelli, G.; Magri, D. Vegetation History of SE Sicily from Feudal Land Management to Post-War Agricultural Industrialization. *Rev. Palaeobot. Palynol.* **2022**, *296*, 104547. [CrossRef]
51. Michelangeli, F.; Di Rita, F.; Celant, A.; Tisnérat-Laborde, N.; Lirer, F.; Magri, D. Three Millennia of Vegetation, Land-Use, and Climate Change in SE Sicily. *Forests* **2022**, *13*, 102. [CrossRef] [PubMed]
52. Schwörer, C.; Morales-Molino, C.; Gobet, E.; Henne, P.D.; Pasta, S.; Pedrotta, T.; van Leeuwen, J.F.N.; Vannière, B.; Tinner, W. Simulating Past and Future Fire Impacts on Mediterranean Ecosystems. *J. Ecol.* **2024**, *112*, 954–970. [CrossRef]
53. Di Rita, F.; Melis, R.T. The Cultural Landscape near the Ancient City of Tharros (Central West Sardinia): Vegetation Changes and Human Impact. *J. Archaeol. Sci.* **2013**, *40*, 4271–4282. [CrossRef]
54. Beffa, G.; Pedrotta, T.; Colombaroli, D.; Henne, P.D.; van Leeuwen, J.F.N.; Süsstrunk, P.; Kaltenrieder, P.; Adolf, C.; Vogel, H.; Pasta, S.; et al. Vegetation and Fire History of Coastal North-Eastern Sardinia (Italy) under Changing Holocene Climates and Land Use. *Veg. Hist. Archaeobot.* **2016**, *25*, 271–289. [CrossRef]
55. Melis, R.T.; Di Rita, F.; French, C.; Marriner, N.; Montis, F.; Serreli, G.; Sulas, F.; Vacchi, M. 8000 years of Coastal Changes on a Western Mediterranean Island: A Multiproxy Approach from the Posada Plain of Sardinia. *Mar. Geol.* **2018**, *403*, 93–108. [CrossRef]
56. Pedrotta, T.; Gobet, E.; Schwörer, C.; Beffa, G.; Butz, C.; Henne, P.D.; Morales-Molino, C.; Pasta, S.; van Leeuwen, J.F.N.; Vogel, H.; et al. 8000 Years of Climate, Vegetation, Fire and Land-Use Dynamics in the Thermo-Mediterranean Vegetation Belt of Northern Sardinia (Italy). *Veg. Hist. Archaeobot.* **2021**, *30*, 789–813. [CrossRef]
57. Reille, M. Contribution Pollen Analytique a l'histoire Tardiglaciaire et Holocene de la Vegetation de la Montagne Corse. Ph.D. Thesis, Université d'Aix-Marseille, Marseille, France, 1975.
58. Di Rita, F.; Ghilardi, M.; Fagel, N.; Vacchi, M.; Warichet, F.; Delanghe, D.; Sicurani, J.; Martinet, L.; Robresco, S. Natural and Anthropogenic Dynamics of the Coastal Environment in Northwestern Corsica (Western Mediterranean) over the Past Six Millennia. *Quat. Sci. Rev.* **2022**, *278*, 107372. [CrossRef]
59. Lestienne, M.; Jouffroy-Bapicot, I.; Leyssenne, D.; Sabatier, P.; Debret, M.; Albertini, P.-J.; Colombaroli, D.; Didier, J.; Hély, C.; Vannière, B. Fires and Human Activities as Key Factors in the High Diversity of Corsican Vegetation. *Holocene* **2020**, *30*, 244–257. [CrossRef]

60. Poher, Y.; Ponel, P.; Médail, F.; Andrieu-Ponel, V.; Guiter, F. Holocene Environmental History of a Small Mediterranean Island in Response to Sea-Level Changes, Climate and Human Impact. *Palaeogeogr. Palaeoclimatol. Palaeoecol.* **2017**, *465*, 247–263. [CrossRef]
61. Picornell-Gelabert, L.; Servera-Vives, G. Landscape Practices and Everyday Life in Domestic Spaces in Bronze Age Mallorca (Balearic Islands): Perspectives for and Archaeology of Fuel and Firewood. *Quat. Int.* **2017**, *431*, 73–89. [CrossRef]
62. Di Domenico, F.; Lucchese, F.; Magri, D. *Buxus* in Europe: Late Quaternary Dynamics and Modern Vulnerability. *Perspect. Plant Ecol. Evol. Syst.* **2012**, *14*, 354–362. [CrossRef]
63. Ninyerola, M.; Sáez, L.; Pérez-Obiol, R. Relating Postglacial Relict Plants and Holocene Vegetation Dynamics in the Balearic Islands Through Field Surveys, Pollen Analysis and GIS Modeling. *Plant Biosyst.* **2007**, *141*, 292–304. [CrossRef]
64. Kaniewski, D.; Marriner, N.; Cheddadi, R.; Morhange, C.; Ontiveros, M.Á.C.; Fornós, J.J.; Giaime, M.; Trichon, V.; Otto, T.; Luce, F.; et al. Recent Anthropogenic Climate Change Exceeds the Rate and Magnitude of Natural Holocene Variability on the Balearic Islands. *Anthropocene* **2020**, *32*, 100268. [CrossRef]
65. Onac, B.P.; Polyak, V.J.; Mitrovica, J.X.; Ginés, J.; Gràcia, F.; Fornós, J.J.; Ginés, A.; Asmerom, Y. Submerged Bridge Constructed at Least 5600 Years Ago Indicates Early Human Arrival in Mallorca Spain. *Commun. Earth Environ.* **2024**, *5*, 457. [CrossRef]
66. Carrión, J.S.; Fernández, S.; González-Sampériz, P.; Gil-Romera, G.; Badal, E.; Carrión-Marco, Y.; López-Merino, L.; López-Sáez, J.A.; Fierro, E.; Burjachs, F. Expected Trends and Surprises in the Lateglacial and Holocene Vegetation History of the Iberian Peninsula and Balearic Islands. *Rev. Palaeobot. Palynol.* **2010**, *162*, 458–475. [CrossRef]
67. Di Rita, F.; Magri, D. An Overview of the Holocene Vegetation History from the Central Mediterranean Coasts. *J. Mech. Eng. Sci.* **2012**, *4*, 35–52. [CrossRef]
68. Buosi, C.; Del Rio, M.; Orrù, P.; Pittau, P.; Scanu, G.G.; Solinas, E. Sea Level Changes and Past Vegetation in the Punic Period (5th–4th Century BC): Archaeological, Geomorphological and Palaeobotanical Indicators (South Sardinia—West Mediterranean Sea). *Quat. Int.* **2017**, *439*, 141–157. [CrossRef]
69. Vella, M.-A.; Andrieu-Ponel, V.; Cesari, J.; Leandri, F.; Pêche-Quilichini, K.; Reille, M.; Poher, Y.; Demory, F.; Delanghe, D.; Ghilardi, M.; et al. Early Impact of Agropastoral Activities and Climate on the Littoral Landscape of Corsica since Mid-Holocene. *PLoS ONE* **2019**, *14*, e0226358. [CrossRef] [PubMed]
70. Di Rita, F.; Lirer, F.; Bonomo, S.; Cascella, A.; Ferraro, L.; Florindo, F.; Insinga, D.D.; Lurcock, P.C.; Margaritelli, G.; Petrosino, P.; et al. Late Holocene Forest Dynamics in the Gulf of Gaeta (Central Mediterranean) in Relation to NAO Variability and Human Impact. *Quat. Sci. Rev.* **2018**, *179*, 137–152. [CrossRef]
71. Jalut, G.; Dedoubat, J.J.; Fontugne, M.; Otto, T. Holocene Circum-Mediterranean Vegetation Changes: Climate Forcing and Human Impact. *Quat. Int.* **2009**, *200*, 4–18. [CrossRef]
72. Pérez-Obiol, R.; Jalut, G.; Julià, R.; Pèlachs, A.; Iriarte, M.J.; Otto, T.; Hernández-Beloqui, B. Mid-Holocene Vegetation and Climatic History of the Iberian Peninsula. *Holocene* **2011**, *21*, 75–93. [CrossRef]
73. Combourieu-Nebout, N.; Peyron, O.; Bout-Roumazeilles, V.; Goring, S.; Dormoy, I.; Joannin, S.; Sadori, L.; Siani, G.; Magny, M. Holocene Vegetation and Climate Changes in the Central Mediterranean Inferred from a High-Resolution Marine Pollen Record (Adriatic Sea). *Clim. Past* **2013**, *9*, 2023–2042. [CrossRef]
74. Cipolla, S.S.; Montaldo, N. On the Impacts of Historical and Future Climate Changes to the Sustainability of the Main Sardinian Forests. *Remote Sens.* **2022**, *14*, 4893. [CrossRef]
75. Magri, D.; Parra, I. Late Quaternary Western Mediterranean Pollen Records and African Winds. *Earth Planet. Sci. Lett.* **2002**, *200*, 401–408. [CrossRef]
76. Di Rita, F.; Magri, D. Holocene Drought, Deforestation and Evergreen Vegetation Development in the Central Mediterranean: A 5500 Year Record from Lago Alimini Piccolo, Apulia, Southeast Italy. *Holocene* **2009**, *19*, 295–306. [CrossRef]
77. Di Rita, F.; Magri, D. The 4.2 Ka Event in the Vegetation Record of the Central Mediterranean. *Clim. Past* **2019**, *15*, 237–251. [CrossRef]
78. Di Rita, F.; Michelangeli, F.; Celant, A.; Magri, D. Sign-Switching Ecological Changes in the Mediterranean Basin at 4.2 Ka BP. *Glob. Planet. Chang.* **2022**, *208*, 103713. [CrossRef]
79. Bond, G.; Showers, W.; Cheseby, M.; Lotti, R.; Almasi, P.; deMenocal, P.; Priore, P.; Cullen, H.; Hajdas, I.; Bonani, G. A Pervasive Millennial-Scale Cycle in North Atlantic Holocene and Glacial Climates. *Science* **1997**, *278*, 1257–1266. [CrossRef]
80. Wirth, S.B.; Glur, L.; Gilli, A.; Anselmetti, F.S. Holocene Flood Frequency across the Central Alps—Solar Forcing and Evidence for Variations in North Atlantic Atmospheric Circulation. *Quat. Sci. Rev.* **2013**, *80*, 112–128. [CrossRef]
81. Le Houedec, S.; Liebrand, D.; Hennekam, R.; Mojtahid, M. Assessing Atmospheric and Oceanic Teleconnections between the Eastern and Western Mediterranean over the Past 8000 Years. *Holocene* **2024**, *34*, 162–174. [CrossRef]
82. Incarbona, A.; Sprovieri, M. The Postglacial Isotopic Record of Intermediate Water Connects Mediterranean Sapropels and Organic-Rich Layers. *Paleoceanogr. Paleoclimatol.* **2020**, *35*, e2020PA004009. [CrossRef]
83. Chiessi, C.M.; Mulitza, S.; Groeneveld, J.; Silva, J.B.; Campos, M.C.; Gurgel, M.H.C. Variability of the Brazil Current during the Late Holocene. *Palaeogeogr. Palaeoclimatol. Palaeoecol.* **2014**, *415*, 28–36. [CrossRef]

84. Dima, M.; Lohmann, G. Conceptual Model for Millennial Climate Variability: A Possible Combined Solar-Thermohaline Circulation Origin for the ~1,500-Year Cycle. *Clim. Dyn.* **2009**, *32*, 301–311. [CrossRef]
85. Berner, K.S.; Koç, N.; Divine, D.; Godtliebsen, F.; Moros, M. A Decadal-scale Holocene Sea Surface Temperature Record from the Subpolar North Atlantic Constructed Using Diatoms and Statistics and Its Relation to Other Climate Parameters. *Paleoceanography* **2008**, *23*, 2006PA001339. [CrossRef]
86. Russell, J.M.; Johnson, T.C.; Talbot, M.R. A 725 Yr Cycle in the Climate of Central Africa during the Late Holocene. *Geology* **2003**, *31*, 677–680. [CrossRef]
87. Fletcher, W.J.; Debret, M.; Goñi, M.F.S. Mid-Holocene Emergence of a Low-Frequency Millennial Oscillation in Western Mediterranean Climate: Implications for Past Dynamics of the North Atlantic Atmospheric Westerlies. *Holocene* **2013**, *23*, 153–166. [CrossRef]
88. Volkov, D.L.; Baringer, M.; Smeed, D.; Johns, W.; Landerer, F.W. Teleconnection between the Atlantic Meridional Overturning Circulation and Sea Level in the Mediterranean Sea. *J. Clim.* **2019**, *32*, 935–955. [CrossRef]
89. Petridi, N.; Polychroni, I.; Hatzaki, M. The Impact of the Atlantic Meridional Overturning Circulation (AMOC) Variability on the Mediterranean Climate. *Environ. Sci. Proc.* **2023**, *26*, 160. [CrossRef]
90. Stuiver, M.; Braziunas, T.F. Atmospheric 14C and Century-Scale Solar Oscillations. *Nature* **1989**, *338*, 405–408. [CrossRef]
91. Damon, P.E.; Jirikowic, J.L. The Sun as a Low-Frequency Harmonic Oscillator. *Radiocarbon* **1992**, *34*, 199–205. [CrossRef]
92. Yu, Z.; Ito, E. The 400-Year Wet-Dry Climate Cycle in Interior North America and Its Solar Connection. In Proceedings of the Proceedings of the Nineteenth Annual Pacific Climate Workshop, Pacific Grove, CA, USA, 3–6 March 2002.
93. Sabatier, P.; Nicolle, M.; Piot, C.; Colin, C.; Debret, M.; Swingedouw, D.; Perrette, Y.; Bellingery, M.-C.; Chazeau, B.; Develle, A.-L.; et al. Past African Dust Inputs in the Western Mediterranean Area Controlled by the Complex Interaction between the Intertropical Convergence Zone, the North Atlantic Oscillation, and Total Solar Irradiance. *Clim. Past* **2020**, *16*, 283–298. [CrossRef]
94. Martín-Chivelet, J.; Muñoz-García, M.B.; Edwards, R.L.; Turrero, M.J.; Ortega, A.I. Land Surface Temperature Changes in Northern Iberia since 4000 Yr BP, Based on δ13C of Speleothems. *Glob. Planet. Chang.* **2011**, *77*, 1–12. [CrossRef]
95. Degeai, J.-P.; Devillers, B.; Dezileau, L.; Oueslati, H.; Bony, G. Major Storm Periods and Climate Forcing in the Western Mediterranean during the Late Holocene. *Quat. Sci. Rev.* **2015**, *129*, 37–56. [CrossRef]
96. Azuara, J.; Sabatier, P.; Lebreton, V.; Jalali, B.; Sicre, M.-A.; Dezileau, L.; Bassetti, M.-A.; Frigola, J.; Combourieu-Nebout, N. Mid- to Late-Holocene Mediterranean Climate Variability: Contribution of Multi-Proxy and Multi-Sequence Comparison Using Wavelet Spectral Analysis in the Northwestern Mediterranean Basin. *Earth-Sci. Rev.* **2020**, *208*, 103232. [CrossRef]
97. Gao, G.; Niu, H.; Song, L.; Wang, J.; Meng, M.; Yang, Z.; Liu, L.; Wei, Y.; Chen, N.; Yu, J.; et al. Solar Forcing and ENSO Regulated Rates of Chang. of Ecosystems in Northeast China since the Last Deglaciation. *Palaeogeogr. Palaeoclimatol. Palaeoecol.* **2023**, *627*, 111728. [CrossRef]
98. Piervitali, E.; Colacino, M. Evidence of Drought in Western Sicily during the Period 1565–1915 from Liturgical Offices. *Clim. Chang.* **2001**, *49*, 225–238. [CrossRef]
99. Vaquero, J.M.; Gallego, M.C.; García, J.A. A 250-Year Cycle in Naked-Eye Observations of Sunspots. *Geophys. Res. Lett.* **2002**, *29*, 58-1–58-4. [CrossRef]
100. Ogurtsov, M.G.; Nagovitsyn, Y.A.; Kocharov, G.E.; Jungner, H. Long-Period Cycles of the Sun's Activity Recorded in Direct Solar Data and Proxies. *Sol. Phys.* **2002**, *211*, 371–394. [CrossRef]
101. Matthews, J.A.; Olaf Dahl, S.; Nesje, A.; Berrisford, M.S.; Andersson, C. Holocene Glacier Variations in Central Jotunheimen, Southern Norway Based on Distal Glaciolacustrine Sediment Cores. *Quat. Sci. Rev.* **2000**, *19*, 1625–1647. [CrossRef]
102. Borgmark, A. Holocene Climate Variability and Periodicities in South-Central Sweden, as Interpreted from Peat Humification Analysis. *Holocene* **2005**, *15*, 387–395. [CrossRef]
103. Dykoski, C.A.; Edwards, R.L.; Cheng, H.; Yuan, D.; Cai, Y.; Zhang, M.; Lin, Y.; Qing, J.; An, Z.; Revenaugh, J. A High-Resolution, Absolute-Dated Holocene and Deglacial Asian Monsoon Record from Dongge Cave, China. *Earth Planet. Sci. Lett.* **2005**, *233*, 71–86. [CrossRef]
104. Swindles, G.T.; Plunkett, G.; Roe, H.M. A Delayed Climatic Response to Solar Forcing at 2800 Cal. BP: Multiproxy Evidence from Three Irish Peatlands. *Holocene* **2007**, *17*, 177–182. [CrossRef]
105. Swindles, G.T.; Patterson, R.T.; Roe, H.M.; Galloway, J.M. Evaluating Periodicities in Peat-Based Climate Proxy Records. *Quat. Sci. Rev.* **2012**, *41*, 94–103. [CrossRef]
106. Di Rita, F. A possible solar pacemaker for Holocene fluctuations of a salt-marsh in southern Italy. *Quat. Int.* **2013**, *288*, 239–248. [CrossRef]
107. Castagnoli, G.C.; Bonino, G.; Della Monica, P.; Taricco, C.; Bernasconi, S.M. Solar Activity in the Last Millennium Recorded in the δ18O Profile of Planktonic Foraminifera of a Shallow Water Ionian Sea Core. *Sol. Phys.* **1999**, *188*, 191–202. [CrossRef]
108. Ma, L.; Vaquero, J.M. New Evidence of the Suess/de Vries Cycle Existing in Historical Naked-Eye Observations of Sunspots. *Open Astron.* **2020**, *29*, 28–31. [CrossRef]

109. Jiang, D.; Lang, X.; Tian, Z.; Ju, L. Mid-Holocene East Asian Summer Monsoon Strengthening: Insights from Paleoclimate Modeling Intercomparison Project (PMIP) Simulations. *Palaeogeogr. Palaeoclimatol. Palaeoecol.* **2013**, *369*, 422–429. [CrossRef]
110. Turney, C.S.M.; Palmer, J.; Hogg, A.; Fogwill, C.J.; Jones, R.T.; Bronk Ramsey, C.; Fenwick, P.; Grierson, P.; Wilmshurst, J.; O'Donnell, A.; et al. Multidecadal Variations in Southern Hemisphere Atmospheric 14C: Evidence against a Southern Ocean Sink at the End of the Little Ice Age CO_2 Anomaly. *Glob. Biogeochem. Cycles* **2016**, *30*, 211–218. [CrossRef]
111. Spiridonov, A.; Balakauskas, L.; Stankevič, R.; Kluczynska, G.; Gedminienė, L.; Stančikaitė, M. Holocene Vegetation Patterns in Southern Lithuania Indicate Astronomical Forcing on the Millennial and Centennial Time Scales. *Sci. Rep.* **2019**, *9*, 14711. [CrossRef] [PubMed]
112. Ron, C.; Chapanov, Y.; Vondrak, J. Solar Excitation of Bicentennial Earth Rotation Oscillations. *Acta Geodyn. Geomater.* **2012**, *9*, 167.
113. Incarbona, A.; Bonomo, S.; Cacho, I.; Lirer, F.; Margaritelli, G.; Pecoraro, D.; Ziveri, P. Solar Forcing for Nutricline Depth Variability Inferred by Coccoliths in the Pre-Industrial Northwestern Mediterranean. *Glob. Planet. Chang.* **2023**, *224*, 104102. [CrossRef]
114. Pinardi, N.; Zavatarelli, M.; Adani, M.; Coppini, G.; Fratianni, C.; Oddo, P.; Simoncelli, S.; Tonani, M.; Lyubartsev, V.; Dobricic, S.; et al. Mediterranean Sea Large-Scale Low-Frequency Ocean Variability and Water Mass Formation Rates from 1987 to 2007: A Retrospective Analysis. *Prog. Oceanogr.* **2015**, *132*, 318–332. [CrossRef]
115. Somot, S.; Houpert, L.; Sevault, F.; Testor, P.; Bosse, A.; Taupier-Letage, I.; Bouin, M.-N.; Waldman, R.; Cassou, C.; Sanchez-Gomez, E.; et al. Characterizing, Modelling and Understanding the Climate Variability of the Deep Water Formation in the North-Western Mediterranean Sea. *Clim. Dyn.* **2018**, *51*, 1179–1210. [CrossRef]
116. Seyfried, L.; Estournel, C.; Marsaleix, P.; Richard, E. Dynamics of the North Balearic Front during an Autumn Tramontane and Mistral Storm: Air–Sea Coupling Processes and Stratification Budget Diagnostic. *Ocean Sci.* **2019**, *15*, 179–198. [CrossRef]
117. Briffa, K.R.; Jones, P.D.; Bartholin, T.S.; Eckstein, D.; Schweingruber, F.H.; Karlén, W.; Zetterberg, P.; Eronen, M. Fennoscandian Summers from Ad 500: Temperature Changes on Short and Long Timescales. *Clim. Dyn.* **1992**, *7*, 111–119. [CrossRef]
118. Loope, W.L.; Arbogast, A.F. Dominance of an ∼150-Year Cycle of Sand-Supply Change in Late Holocene Dune-Building along the Eastern Shore of Lake Michigan. *Quat. Res.* **2000**, *54*, 414–422. [CrossRef]
119. Raspopov, O.M.; Dergachev, V.A.; Esper, J.; Kozyreva, O.V.; Frank, D.; Ogurtsov, M.; Kolström, T.; Shao, X. The Influence of the de Vries (∼200-Year) Solar Cycle on Climate Variations: Results from the Central Asian Mountains and Their Global Link. *Palaeogeogr. Palaeoclimatol. Palaeoecol.* **2008**, *259*, 6–16. [CrossRef]
120. Hou, G.; E, C.; Liu, X.; Zeng, F. Reconstruction of Integrated Temperature Series of the Past 2000 Years on the Tibetan Plateau with 10-Year Intervals. *Theor. Appl. Climatol.* **2013**, *113*, 259–269. [CrossRef]
121. Huang, C.; Yang, Y.; Chen, F.; Kong, D.; Xu, J.; Chen, C.; Zhu, Q.; Huang, X. External Forcing Mechanisms Controlling the Qiongdong Upwelling in the Northern South China Sea during the Holocene. *Glob. Planet. Chang.* **2023**, *220*, 104021. [CrossRef]
122. Ptitsyna, N.G.; Demina, I.M. Frequency Modulation as a Cause of Additional Branches of the Gleissberg Cycle in Solar Activity. *Geomagn. Aeron.* **2021**, *61*, S48–S61. [CrossRef]
123. Azharuddin, S.; Govil, P.; Singh, A.D.; Mishra, R.; Shekhar, M. Solar Insolation Driven Periodicities in Southwest Monsoon and Its Impact on NE Arabian Sea Paleoceanography. *Geosci. Front.* **2019**, *10*, 2251–2263. [CrossRef]
124. Poore, R.Z.; Dowsett, H.J.; Verardo, S.; Quinn, T.M. Millennial- to Century-Scale Variability in Gulf of Mexico Holocene Climate Records. *Paleoceanography* **2003**, *18*, 1048. [CrossRef]
125. Nogué, S.; de Nascimento, L.; Froyd, C.A.; Wilmshurst, J.M.; de Boer, E.J.; Coffey, E.E.D.; Whittaker, R.J.; Fernández-Palacios, J.M.; Willis, K.J. Island Biodiversity Conservation Needs Palaeoecology. *Nat. Ecol. Evol.* **2017**, *1*, 0181. [CrossRef]

Disclaimer/Publisher's Note: The statements, opinions and data contained in all publications are solely those of the individual author(s) and contributor(s) and not of MDPI and/or the editor(s). MDPI and/or the editor(s) disclaim responsibility for any injury to people or property resulting from any ideas, methods, instructions or products referred to in the content.